journal of the international meteor organization

WGN

44:2
april 2016

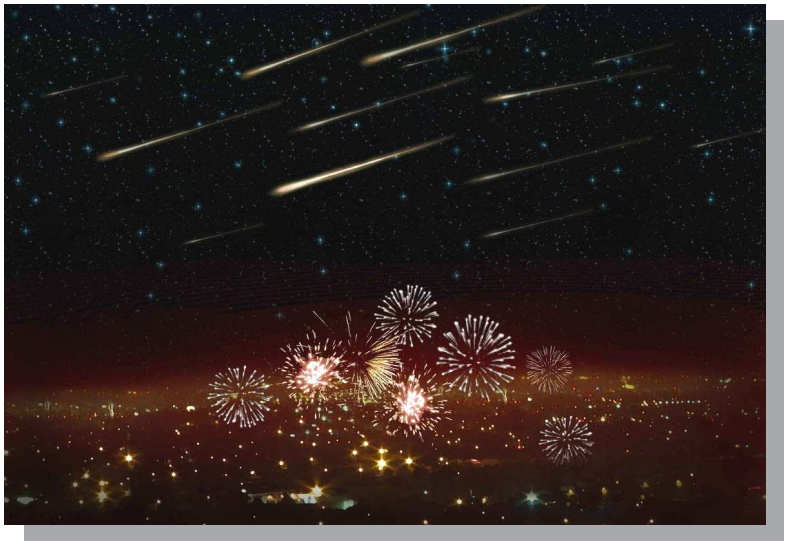

Definitions of meteoroid, asteroid, and related terms
Volantids surprise southern-hemisphere observers on New-Year's Eve
Observation error propagation incorporated in UFO suite
November–December video meteors

ISSN 1016-3115

WGN Vol. 44, No. 2, April 2016, pp. 31 – 56

Administrative

Meteor science

Preliminary results

Front cover photo

New Year's Eve meteor shower (see inside for a paper about the Volantids). Illustration: Danielle Futselaar/SETI Institute.

Writing for WGN

This Journal welcomes papers submitted for publication. All papers are reviewed for scientific content, and edited for English and style. Instructions for authors can be found in WGN **31:4**, 124–128, and at `http://www.imo.net/docs/writingforwgn.pdf` .

Legal address

International Meteor Organization, Jozef Mattheessensstraat 60, 2540 Hove, Belgium.

About the definition of meteoroid, asteroid, and related terms

Jiří Borovička[1]

The terms meteoroid, meteor, meteorite, and asteroid are commonly used but poorly defined. The last official definitions in meteoric astronomy date back to 1961 and are no longer adequate. For that reason the discussion about new definitions was started within the Commission 22 of the International Astronomical Union. I present here the current proposal. Readers are welcome to comment about it.

Received 2016 March 23

1 Motivation

As recently as 25 years ago, asteroids and meteoroids were totally distinct classes of objects. All known asteroids were larger than 100 meters. The first asteroid with absolute magnitude $H > 23$, which nearly corresponds to diameter of 100 meters, was discovered in 1990 (asteroid 1990 UN). During that same period the brightest fireballs observed in the Earth's atmosphere were caused by meteoroids of sizes a few meters at maximum. Nothing was known about bodies of intermediate sizes of $\sim 5 - 100$ m, except for the 1908 Tunguska event, estimated to be caused by a ~ 60 m body, where, however, the available data were very limited.

Today, the situation is quite different. According to the JPL Small-Body Database[a] eight cataloged asteroids have $H > 31$, corresponding to sizes about 2 meters or less. The dimmest asteroid 2008 TS_{26} has $H = 33.2$, i.e. a size between 0.6 to 1.3 m, depending on its actual albedo. These sizes are smaller than that of many meteoroids whose entries into the atmosphere were observed as fireballs. The clear distinction between asteroids and meteoroids according to size has therefore completely disappeared. These terms are nowadays used mostly depending on the method of observation or general context. Sometimes, different terms are used for the same object. The most well-known case is 2008 TC_3. The object was discovered telescopically as an asteroid. The following day it impacted the Earth, the corresponding fireball was observed, and meteorites, named Almahata Sitta, were recovered (Jenniskens et al., 2009). During the fireball phase, the object was often referred to as a meteoroid. Another confusing case was the Chelyabinsk event of February 15, 2013, which caused widespread damage and was produced by a ~ 19 m body. The body was observed only during atmospheric entry but because of its size it could easily have been called asteroid.

Astronomers working in the fields of meteors and small solar system bodies understand the situation well and usually do not feel the necessity of exact definitions. However, we need definitions for the general public, teachers, and scientists from other fields. The definitions will also serve for naming generic bodies of certain size. People expect that an exact science like astronomy would use precisely defined terms.

Although some meteoroids are of cometary origin, the most problematic distinction is between meteoroids and asteroids. Historically, these terms are related to the method of observation. Asteroids are star-like objects seen in the telescope, while meteoroids are bodies causing meteors in the atmosphere. Both, nevertheless, are solid objects orbiting the Sun and they differ mainly by size (and, of course, spatial density, i.e. number of objects in a given volume). We can ask if there is any physical boundary which could be used to define the difference between asteroids and meteoroids.

There is in fact a quite sharp transition in rotational properties as a function of size. As described e.g. by Pravec and Harris (2000) or Warner and Harris (2011), almost all asteroids larger than about 200 meters have rotational periods longer than 2 hours. Smaller bodies have a wide range of rotational periods, sometimes only of the order of minute. Moreover, as pointed out by Harris and D'Abramo (2015), the size-frequency distribution of Near Earth Objects suggest that bodies smaller and bodies larger than 200 meters may represent two different populations. The most probable explanation of rotational properties is that asteroids in the size range 200 m – 10 km are mostly strengthless gravitational aggregates (rubble piles). Smaller bodies tend to be monolithic. One might then have physical grounds for setting the boundary between meteoroids and asteroids at 200 meters. However, such a definition would contradict current and past usages. For historical reasons the boundary has been implicitly assumed to be somewhere in the 1 – 10 meter range. I therefore recommend that the boundary be set by agreement, without physical grounds.

It is also desirable to define the lower limit of meteoroid size, i.e. the boundary between meteoroid and dust particle. It is well known that small particles do not ablate in the atmosphere since they are decelerated before the temperature needed for ablation is reached. They therefore do not produce a meteor phenomenon. It will be natural to use the term meteoroids only for particles able to produce meteors. The limit for ablation is somewhere around 30 micrometers but depends on many parameters such as entry speed and angle, structure and composition of the particle, and density profile of the atmosphere.

In other contexts, the term dust is used for wide range of particle sizes. Interplanetary dust particles (IDPs) collected in the stratosphere have typically sizes

[1]Astronomical Institute of the Czech Academy of Sciences, Fričova 298, CZ-25165 Ondřejov, Czech Republic.
E-mail: jiri.borovicka@asu.cas.cz

IMO bibcode WGN-442-borovicka-definitions
NASA-ADS bibcode 2016JIMO...44...31B

[a]http://ssd.jpl.nasa.gov/sbdb_query.cgi

10 – 15 μm, but so-called cluster IDPs up to 600 μm in size do not show obvious signs of ablation caused during entry (F. Rietmeijer, priv. comm.). Cometary dust tails are mostly formed by micron-sized particles, although the mass loss of comets is dominated by larger (cm-sized) boulders (Fulle, 2004). The typical size of zodiacal dust is most probably 30 – 100 μm (Nesvorný et al., 2010; Janches et al., 2015).

Returning to Earth, there is a maximum rate of influx of particles into Earth's atmosphere which occurs at particle sizes 100 μm (Mathews et al., 2001). It would be not practical to define the boundary between two classes of objects at the maximum influx. Hundred-micron particles ablate in the atmosphere and are easily detected as meteors by powerful radars (provided that they do not have a very low speed). They should therefore be called meteoroids. Taking into account only rounded values, the dust-meteoroid boundary is most easily set at 10 microns. Alternatively, the value 30 μm can be used. Such definition will still leave most zodiacal particles as meteoroids. An even stronger contradiction is found in cometary dust trails, which are formed mostly by cm-sized bodies, i.e. meteoroids. Nevertheless, it is perhaps natural to call remotely observed assemblies of meteoroids that are not resolved individually as dust objects.

2 Existing definitions

In 1961, IAU Commission 22 adopted *Basic Definitions in Meteoric Astronomy.* They were published e.g. by Millman (1961). The boundaries discussed above were only vaguely defined, which caused no problems at that time. Moreover, the 1961 definitions are in contradiction with the current usage of some terms. We will present and discuss the most important 1961 definitions here.

Meteoroid was defined as *a solid object moving in interplanetary space, of a size considerably smaller than an asteroid and considerably larger than an atom or molecule.* Here the boundary with asteroids was not defined and no space was left for dust particles. Moreover, the term meteoroid was used exclusively for bodies in interplanetary space. Nowadays it is also used for the solid objects during their atmospheric entry.

Meteor was defined as *in particular, the light phenomenon which results from the entry into the Earth's atmosphere of a solid particle from space; more generally, as a noun or an adjective, any physical object or phenomenon associated with such an event.* As noted above, meteor is now used only for the phenomenon, not for the physical object. Moreover, though the emitted light remains crucial, the term is also used for other associated phenomena, e.g. sonic waves and ionization detected by radars.

Meteorite was defined as *any object defined under meteoroid which has reached the surface of the Earth without being completely vaporized.* Recently, meteorite-like objects were found in situ on the Martian surface. Thus, it seems reasonable to refer to an interplanetary object that reached a planetary surface after ablation in the planetary atmosphere as a meteorite. It seems also reasonable to call the object a meteorite starting from the moment when it was formed, i.e. when meteoroid ablation stopped, rather than from the moment when it reached the surface.

Fireball was defined as *a bright meteor with luminosity which equals or exceeds that of the brightest planets.*

Micrometeorite was defined as *a very small meteorite or meteoritic particle with a diameter in general less than a millimeter.*

Meteoric or meteoritic ***dust*** was defined as *finely divided solid matter, with particle sizes in general smaller than micrometeorites.* This definition was obviously intended only for dust of cosmic origin found on the Earth.

Other 1961 definitions, such as those of meteor trajectory, radiant, absolute magnitude, wake, shower or stream are not discussed here. They remain valid or need only minor adjustments.

More recently, Beech and Steel (1995) proposed meteoroid to be defined as any natural solid objects moving in space and having a size between 100 μm and 10 m. Rubin and Grossman (2010), on the other hand, proposed the limits 10 μm to 1 meter. They also proposed a meteorite to be defined as a natural, solid object larger than 10 μm in size, derived from a celestial body, that was transported by natural means from the body on which it formed to a region outside the dominant gravitational influence of that body and that later collided with a natural or artificial body larger than itself (even if it is the same body from which it was launched). This definition would mean that for almost any collision in space, the smaller object would be called meteorite.

3 Proposal of new definitions

The inadequacy of the existing official definitions led the Commission 22 of the International Astronomical Union to establish a working committee with the aim to prepare a proposal of new definitions. The members of the committee were Jiří Borovička, Guy Consolmagno, Tadeusz Jopek, Asta Pellinen-Wannberg, Chris Peterson, John Plane, Frans Rietmeijer, and Giovanni Valsecchi. The proposal of the committee has two parts: Definitions of fundamental terms and Explanatory remarks, which also contain secondary definitions. The proposal is intended for natural (not man-made) solar system objects. The definitions of fundamental terms were proposed as follows:

Meteor is the light and associated phenomenon (heat, shock, ionization), which results from the entry of a solid object from space into a gaseous atmosphere.

Meteoroid is a solid object of a diameter between 30 μm and 1 meter moving in, or coming from, interplanetary space.

Dust is finely divided solid matter, with particle sizes in general smaller than meteoroids, moving in, or coming from, interplanetary space.

Asteroid is a solid object of a diameter larger than 1 meter and smaller than a dwarf planet moving in or coming from interplanetary space and showing no activity (i.e. a release of gas, dust or meteoroids).

Comet is a solid object of a diameter larger than 1 meter and smaller than a dwarf planet moving in or coming from interplanetary space and showing activity (i.e. a release of gas, dust or meteoroids).

Meteorite is any solid object that survived the meteor phase in a gaseous atmosphere without being completely vaporized.

Meteoric smoke is solid matter that has condensed in a gaseous atmosphere from material vaporized during the meteor phase.

The explanatory remarks, comments and secondary definitions (in bold) were proposed as follows:

Remarks to ***meteor***

- The meteor phenomenon can be caused by a meteoroid, an asteroid, a comet or any particle with the appropriate combination of velocity, mass and mean-free-path of a planetary atmosphere.
- Meteors can occur on any planet or planetary moon having sufficiently dense atmosphere to vaporize incoming meteoroids at least partly during their atmospheric passage.
- The phenomena caused by meteoroids being vaporized in the vicinity of the Sun due to solar heat are not called meteors because the mechanism of vaporization is different.
- The radiation phenomenon accompanying a direct meteoroid hit on the surface of a body without an atmosphere is not called meteor but **impact flash**.
- Meteor brighter than absolute magnitude −4 can be called **bolide** or **fireball**.
- Meteor brighter than absolute magnitude −17 can be called **superbolide**.

Remark to ***meteoroid***

- In the context of meteor observation, any object causing a meteor can be termed a meteoroid, irrespective of size.

Remark to ***asteroid***

- In the context of asteroid observation, any object observed telescopically and having asteroidal appearance, can be called an asteroid, irrespective of size.

Remarks to ***dust***

- Dust in the solar system is observed e.g. as the **zodiacal dust cloud**, including **zodiacal dust bands**, and **cometary dust tails**. **Cometary dust trails**, on the other hand, contain larger particles, which, when referred to individually, should be called meteoroids.
- Small dust particles do not give rise to the meteor phenomenon when they enter planetary atmosphere. Being only heated below the melting point, they sediment to the ground more or less unaffected. When collected in the atmosphere, they are called **interplanetary dust particles** (IDPs).
- Small (typically micron-size) non-vaporized remnants of ablating meteoroids can be called **meteoritic dust**. They can be observed e.g. as **dust trails** in the atmosphere after the passage of a bolide.

Remarks to ***meteorite***

- A meteoroid in the atmosphere becomes a meteorite after the ablation stops and the object continues on **dark flight** to the ground.
- A meteorite smaller than 1 millimeter can be called **micrometeorite**. Micrometeorites do not have the typical structure of a fresh meteorite – unaffected interior and fusion crust.
- Foreigh objects on the surfaces of atmosphereless bodies are not called meteorites (i.e. there is no meteorite without meteor).

Remark to ***meteoric smoke***

- The sizes of meteoric smoke particles (MSPs) is in the sub-100 nm range.

Dual nomenclature of the same object (asteroid/meteoroid) is therefore explicitly allowed. The term can be chosen according to the context. This is a common practice also for other terms (e.g. asteroid/comet or asteroid/dwarf planet in case of Ceres) and causes no problems. On the other hand, if strict definitions are needed, they are provided.

4 Further prospects

The main ideas of this article were presented by the author at the meeting of IAU Division F during the General Assembly in Honolulu in August 2015. It was acknowledged that new definitions would be useful. IAU is the right body to adopt the definitions, nevertheless, more time for discussion is needed. The proposal will be discussed at the next meeting of IAU Commission F1 (the successor of Commission 22), which will be held during the Meteoroids 2016 conference in Noordwijk in June 2016. If everything goes well, new definitions could be adopted by Commission F1 or Division F before or during the next General Assembly in 2018. The purpose of this article is to stimulate discussion also among the IMO members. Comments and suggestions can be sent to the author by e-mail.

Acknowledgement

I thank G. Consolmagno and F. Rietmeijer for improving the style of this article.

References

Beech M. and Steel D. (1995). "On the definition of the term meteoroid". *Quarterly J. Royal Astron. Soc.*, **36**, 281–284.

Fulle M. (2004). "Motion of cometary dust". In Festou M. C., Keller H. U., and Weaver H. A., editors, *Comets II*, Tucson. Univ. Arizona Press, pages 565–575.

Harris A. W. and D'Abramo G. (2015). "The population of near-Earth asteroids". *Icarus*, **257**, 302–312.

Janches D., Swarnalingam N., Plane J. M. C., Nesvorný D., Feng W., Vokrouhlický D., and Nicolls M. J. (2015). "Radar detectability studies of slow and small zodiacal dust cloud particles: II. A study of three radars with different sensitivity". *Astrophys. J.*, **807:1**, 13.

Jenniskens P., Shaddad M. H., Numan D., and et al. (2009). "The impact and recovery of asteroid 2008 TC3". *Nature*, **458**, 485–488.

Mathews J. D., Janches D., Meisel D. D., and Zhou Q. H. (2001). "The micrometeoroid mass flux into the upper atmosphere: Arecibo results and a comparison with prior estimates". *Geophys. Res. Lett.*, **28**, 1929–1932.

Millman P. M. (1961). "Meteor news. A report on meteor terminology". *J. Royal Astron. Soc. Canada*, **55**, 265–267.

Nesvorný D., Jenniskens P., Levison H. F., Bottke W. F., Vokrouhlický D., and Gounelle M. (2010). "Cometary origin of the zodiacal cloud and carbonaceous micrometeorites. Implications for hot debris disks". *Astrophys. J.*, **713**, 816–836.

Pravec P. and Harris A. W. (2000). "Fast and slow rotation of asteroids". *Icarus*, **148**, 12–20.

Rubin A. E. and Grossman J. N. (2010). "Meteorite and meteoroid: New comprehensive definitions". *Meteorit. Plan. Sci.*, **45**, 114–122.

Warner B. D. and Harris A. W. (2011). "Using sparse photometric data sets for asteroid lightcurve studies". *Icarus*, **216**, 610–624.

Handling Editor: Javor Kac
This paper has been typeset from a LaTeX file prepared by the author.

Letter — The CMN catalogue of orbits for 2013

Croatian Meteor Network [1]

The Croatian Meteor Network (CMN) has released its catalogue of orbits for 2013. The catalogue contains 3422 orbits. It can be accessed from the CMN download page:
`http://cmn.rgn.hr/downloads/downloads.html`

IMO bibcode WGN-442-cmn-letter
NASA-ADS bibcode 2016JIMO...44L..34C

[1]Email: `cmn@rgn.hr`

Meteor science

A surprise southern hemisphere meteor shower on New-Year's Eve 2015: the Volantids (IAU#758, VOL)

Peter Jenniskens[1], *Jack Baggaley*[2], *Ian Crumpton*[3], *Peter Aldous*[4], *Peter S. Gural*[1], *Dave Samuels*[1], *Jim Albers*[1], *and Rachel Soja*[5]

A new 32-camera CAMS network in New Zealand, spread over two stations on South Island, has detected a high southern declination shower that was active on New Year's Eve, 2015 December 31. During the observing interval from $09^{\rm h}12^{\rm m}$–$15^{\rm h}45^{\rm m}$ UT, 21 out of 59 detected meteors radiated from the constellation of Volans, the flying fish, with a geocentric radiant at RA = $122\overset{\circ}{.}9 \pm 4\overset{\circ}{.}7$, Dec = $-71\overset{\circ}{.}9 \pm 1\overset{\circ}{.}9$, and speed $V_g = 28.4 \pm 1.5$ km/s. The new year arrived in New Zealand at $11^{\rm h}00^{\rm m}$ UT. Two more were detected the next night. No activity from this shower was observed the year prior. The meteoroids move in a 48°-inclined Jupiter-family comet orbit. The parent body has not yet been identified.

Received 2016 February 17

1 Introduction

Meteor showers in the southern hemisphere are relatively poorly studied. Early visual meteor observers derived shower radiants from plotted trajectories, results of which were summarized by McIntosh (1935). Later, Jeff Wood led an effort by the N.A.P.O.-Meteor Section around Perth, Australia, to systematically observe known meteor showers, mapping their activity over many years. Results are summarized in Jenniskens (2006).

In the 1960's, radar observations mapped meteor showers in works by Clifford Ellyet and Colin Keay in Christchurch, New Zealand (Ellyett & Roth, 1955; Ellyett et al., 1961), and Graham Elford at Adelaide, Australia (Nilsson, 1964; Gartrell & Elford, 1975). Poole (1995) observed from South Africa. AMOR, a later high-power narrow-beam radar in Christchurch, focused on the smaller meteoroids that dominate the mass influx, but proved less effective at detecting meteoroid streams (Galligan, 2003; Galligan & Baggaley, 2005; Jenniskens, 2006).

More recently, single station radar observations from Davis Station, Antarctica, and Darwin, Australia, detected 37 meteor showers (Younger et al., 2009). Even more results will soon come from a systematic radar survey conducted with the Southern Argentina Agile Meteor Radar (SAAMER) at the southern most tip of Argentina, an instrument similar to CMOR in Canada (Janches et al., 2013; Janches et al., 2015).

Southern hemisphere meteor showers were mapped also by small, temporary, video observation projects (e.g., Jopek et al., 2010) and from mining the IMO Video Meteor Database, which contains more continuous single-station observations from three Australian cameras between 2001 and 2012 (Molau & Kerr, 2014). Radar and video data are complimentary in many ways because they are sensitive to particles of different speed and mass.

Since September of 2014, we have conducted a video-based meteor shower survey from New Zealand, using the Cameras for Allsky Meteor Surveillance (CAMS) technology. Here, we introduce this new network and report on what appears to be a meteor outburst from a previously unknown shower active during New Year's Eve on 2015 December 31.

2 CAMS New Zealand

New Zealand was chosen as the site for a southern hemisphere meteor shower survey because of its high southern latitude of about −44°. This makes it possible to detect night-time southern declination showers efficiently. With support of the Department of Physics and Astronomy, University of Canterbury, two stations were established on South Island at Geraldine (44 °08756S, 171 °24155E, +143 m) and West Melton (43 °49901S, 172 °40738E, +78 m) (Figure 1).

Each station has 16 cameras mounted in a fiberglass box with an optical glass window, much like the CAMS network in California (Jenniskens et al., 2011). With the advent of faster desktop computers and reasonable cost of 16-channel video frame grabbers (the Sensoray 817 PCI-x1 board), the technology was available to permit all the cameras at one station to be run through a single computer using the basic CAMS processing approach. This presented a challenge in dealing with the asynchronous nature of the camera frame ingest, performing the CAMS custom compression on all 16 video channels, and executing the detection process in the available time. Since the latter could not be done fast enough to keep up with the incoming data stream, a multi-threaded restructuring of the CAMS software process was necessary. The redesign gave high priority to the capture, compression and file writing threads of the streaming data, with separate daughter processes launched at low priority to perform detection

[1]SETI Institute, Mountain View, California.
Email: petrus.m.jenniskens@nasa.gov
[2]University of Canterbury, Christchurch, New Zealand.
[3]Canterbury Astronomical Society, West Melton, New Zealand.
[4]Geraldine Observatory, Geraldine, New Zealand.
[5]Institut für Raumfahrtsysteme, Universität Stuttgart, Stuttgart, Germany.

IMO bibcode WGN-442-jenniskens-volantids
NASA-ADS bibcode 2016JIMO...44...35J

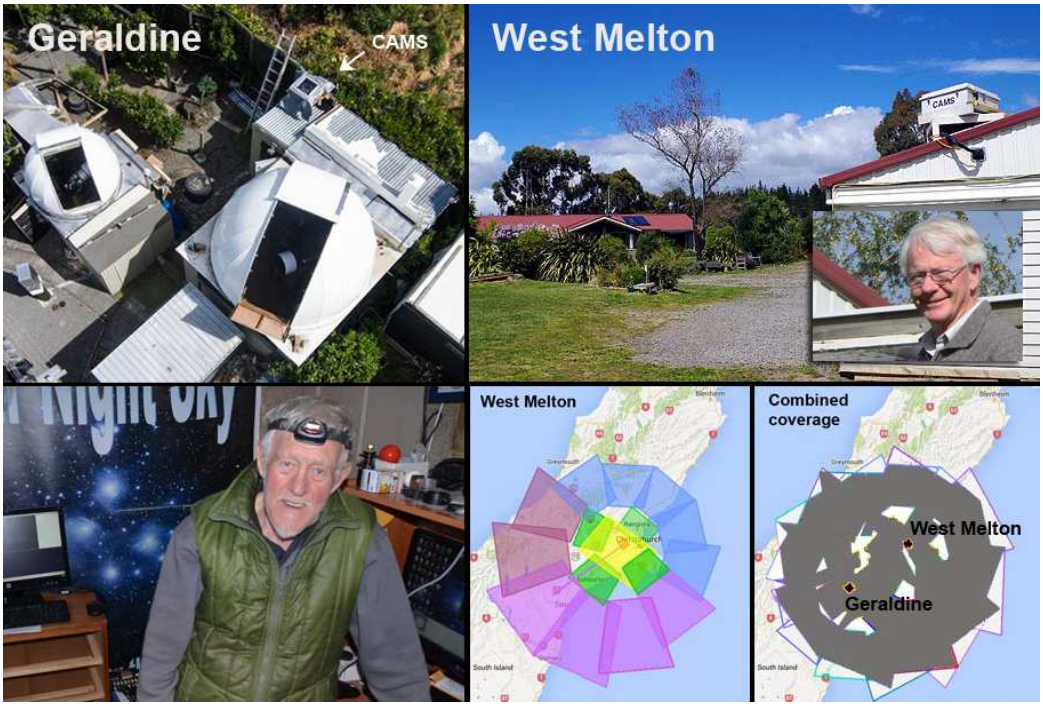

Figure 1 – The Geraldine station and operator Peter Aldous next to the CAMS computer inside his observatory (left) and the West Melton station with an inset showing operator Ian Crumpton (right). The maps to the lower right show the layout of the West Melton cameras (left), while the gray areas show the effective surface area that is covered by both stations simultaneously (right).

and archiving of potential meteor tracks. To handle the multi-threading and processing bandwidth throughput, each computer was chosen to have an i7-4770 quad-core processor. With this setup, no frames are dropped on any of the 16 video channels and the detection processing wraps up later in the morning after capturing is halted due to twilight.

The astrometric data for each camera's field of view, photometric star calibration fits, and the candidate detection track histories on a per interleaved field basis, are submitted to the SETI Institute in California. The two-station events are spatially and temporally combined, reduced to atmospheric trajectories, presented to an analyst for acceptance/quality control, and finally meteoroid orbits are calculated.

Unlike the CAMS California based system, the New Zealand cameras do not fully cover the sky at high elevations as the design/cost limited the number of cameras at each site to sixteen, leaving small gaps in the sky coverage area. Nevertheless, a significant surface area is monitored, half of which is over land in the northern part of South Island, while the remainder is over the Pacific Ocean (Figure 1).

3 Results

First light for CAMS New Zealand was on 2014 September 11, when 62 good trajectories were measured. The detection rate is about 50 meteors per night in a clear night. Locations in New Zealand's South Island have generally less favorable weather conditions than parts of Australia or South Africa, but the majority of nights proved to be at least partially clear.

In 2015 December, the 32-camera CAMS New Zealand network measured 574 meteors from 21 nights. In that same month, the 78-camera CAMS network in California detected 6 355 meteors, in part due to the strong Geminid shower, while the 52-camera CAMS BeNeLux collected 1 589, the 2-camera CAMS Florida added 232, and the 5-camera CAMS Mid-Atlantic added 68.

The combined data are shown in Figure 2, plotted in sun-centered coordinates of ecliptic longitude and latitude (for radiants in right ascension and declination, see Figure 3 below). The core of the Puppid-Velid I Complex (#255 PUV) is found at a relatively high $\sim -51°$ southern declination, centered around solar longitude $\lambda_\odot \sim 258°$, which also translates to a high southern ecliptic latitude (yellow in Figure 2). The early component of this, the e-Velids (#746, EVE), are at $-45°$ declination (at $\lambda_\odot \sim 251°$). The California and Florida networks reach down to a southern declination of about $-53°$ and captured this latter shower (Jenniskens et al., 2016). Showers even further south are detected only by the CAMS New Zealand stations. Of all measured CAMS New Zealand meteor radiants so far, 17% have declinations south of $-53°$.

Figure 2 shows a group of meteors at $-79°$ declination, marked with an arrow. All but one of these were detected in the night of 2015 December 31, between 09^h12^m and 15^h45^m UT. Results from that night are shown by crosses in Figure 3, when 21 out of 59 meteors (36%) belonged to this shower (arrow). Meteors were spread throughout the night, with good rates around 10^h15^m UT. Because of local daylight savings time, the new year started at 11^h00^m UT.

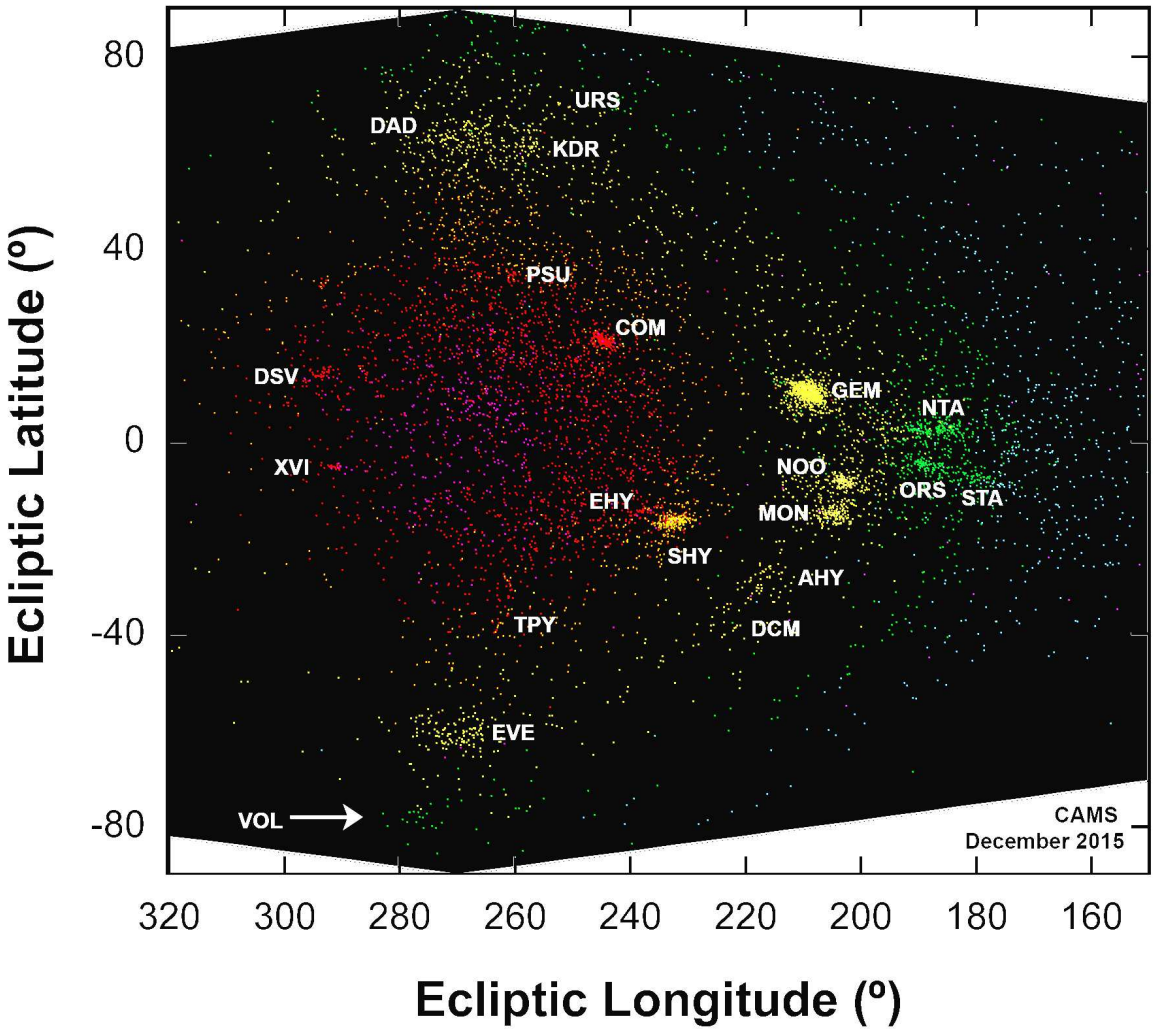

Figure 2 – The combined CAMS network results for December 2015, with the radiants plotted in ecliptic coordinates, corrected for the daily radiant drift by ecliptic longitude $\Delta\lambda = 1^\circ$/day, and ecliptic latitude $\Delta\beta = 0^\circ$/day. Blue are slow meteors, red are fast. The Volantids (VOL) are marked by an arrow: all but one of these meteors appeared on December 31. Other showers in this graph include the Puppid-Velid I Complex just above the Volantids, including the e-Velids (EVE), the established Geminids (GEM), Ursids (URS), November Orionids (NOO), December Monocerotids (MON), Northern and Southern Taurids (NTA, STA), Southern χ-Orionids (ORS), σ-Hydrids (SHY), η-Hydrids (EHY), Comae Berenicids (COM), December α-Draconids (DAD), December κ-Draconids (KDR), December χ-Virginids (XVI), and December σ-Virginids (DSV), as well as the now confirmed θ-Piscids (TPY) and December Canis Majorids (DCM).

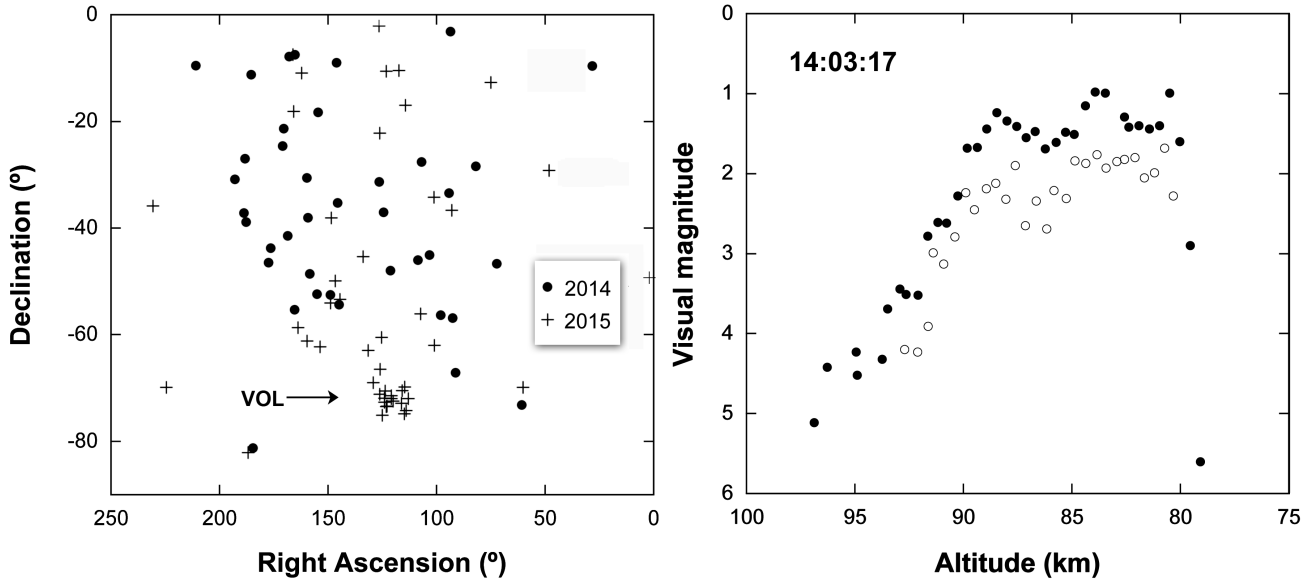

Figure 3 – Left: radiants measured on 2015 December 31 (+), compared to those of 2014 December 31 and 2015 January 1 (•). Right: a typical lightcurve, Volantid of 14:03:17 UT (Geraldine: •; West Melton: ○).

Time (UT)	$\lambda_\odot$ (°)	RA_∞ † (°)	Dec_∞ (°)	V_∞ (km/s)	a_1 (km/s)	a_2 (1/s)	H_b (km)	H_e (km)	Q (°)	M_v (magn.)	F	Shape ††
$09^h22^m00^s$	279.1596	116.50 ± 0.55	-71.76 ± 0.06	32.49 ± 0.11	0.08 ± 0.00	8.26 ± 0.11	98.0	82.4	58.5	+1.5	0.76	U,sl
$09^h31^m28^{s*}$	279.1663	120.81 ± 0.04	-74.34 ± 0.05	32.01 ± 0.12	0.00 ± 0.00	13.52 ± 0.03	128.4	71.7	5.7	−1.7	0.69	U
$09^h51^m55^s$	279.1808	122.79 ± 0.31	-70.50 ± 0.07	32.15 ± 0.07	0.00 ± 0.04	0.09 ± 0.11	95.7	76.0	41.8	−0.9	0.68	U,sl
$10^h02^m44^s$	279.1884	113.36 ± 0.87	-71.95 ± 0.13	31.26 ± 0.21	0.09 ± 0.05	0.13 ± 0.13	93.8	80.7	40.7	+2.1	0.65	U,sl
$10^h15^m17^s$	279.1973	119.30 ± 0.30	-72.38 ± 0.16	28.49 ± 0.24	0.24 ± 0.07	0.09 ± 0.07	97.4	85.0	40.8	+0.7	0.73	U,sl
$10^h17^m37^{s*}$	279.1990	110.50 ± 1.17	-72.83 ± 0.14	26.11 ± 0.31	0.00 ± 0.04	0.91 ± 0.11	94.4	84.0	31.9	+1.1	0.63	U,sl
$10^h18^m35^{s*}$	279.1996	111.53 ± 2.20	-73.64 ± 0.31	28.60 ± 0.19	0.00 ± 0.05	0.17 ± 0.19	92.7	83.5	34.4	+2.3	0.43	U,sl
$10^h32^m25^s$	279.2094	118.30 ± 0.43	-70.96 ± 0.09	30.36 ± 1.56	0.12 ± 0.05	0.28 ± 2.57	98.3	81.3	60.4	+0.3	0.62	U,sl
$10^h34^m23^s$	279.2108	117.68 ± 0.91	-70.31 ± 0.33	27.39 ± 0.64	0.00 ± 0.06	0.17 ± 0.08	93.4	87.4	88.8	+2.9	0.58	U,sl
$10^h53^m03^s$	279.2240	113.32 ± 0.68	-68.79 ± 0.41	30.55 ± 0.33	0.05 ± 0.03	0.02 ± 0.12	96.7	84.2	32.8	+0.9	0.65	U,sl
$10^h59^m05^{s*}$	279.2283	117.37 ± 5.26	-65.54 ± 0.14	30.52 ± 0.16	0.02 ± 0.08	0.17 ± 0.17	91.9	79.1	54.0	+1.3	0.26	U
$11^h18^m57^{s*}$	279.2424	134.11 ± 7.31	-78.00 ± 2.11	31.71 ± 6.03	0.66 ± 0.49	1.85 ± 0.80	96.0	86.8	35.5	+2.4	0.86	U,sl
$11^h56^m44^s$	279.2691	125.13 ± 0.48	-65.54 ± 0.14	30.52 ± 0.16	0.00 ± 0.02	0.11 ± 0.07	95.7	84.9	85.8	+1.2	0.68	U,sl
$12^h04^m33^s$	279.2746	127.94 ± 0.93	-67.92 ± 0.13	29.31 ± 0.46	0.03 ± 0.05	0.12 ± 1.27	94.2	83.9	36.8	+2.8	0.48	U
$12^h37^m55^s$	279.2982	114.16 ± 0.46	-70.83 ± 0.10	28.88 ± 0.25	0.01 ± 0.01	0.41 ± 0.07	95.5	78.0	45.3	−0.3	0.97	U,fr
$12^h45^m36^s$	279.3037	123.21 ± 0.35	-72.11 ± 0.27	30.04 ± 0.07	0.00 ± 0.01	0.27 ± 0.07	97.1	82.8	30.1	+1.8	0.59	U,sl
$13^h02^m51^s$	279.3159	124.17 ± 0.29	-69.52 ± 0.12	30.49 ± 0.36	0.06 ± 0.04	0.04 ± 0.02	98.2	83.3	70.9	+1.2	0.62	U,sl
$13^h17^m38^s$	279.3264	117.22 ± 0.73	-69.56 ± 0.14	31.39 ± 0.19	0.10 ± 0.05	0.07 ± 0.09	93.6	80.6	40.4	+2.0	0.82	U,sl
$13^h41^m45^s$	279.3434	125.39 ± 0.27	-70.91 ± 0.06	31.32 ± 0.11	0.04 ± 0.06	0.32 ± 0.18	99.6	77.8	65.0	−0.1	0.74	U,sl
$13^h54^m42^{s*}$	279.3526	125.03 ± 4.59	-71.57 ± 0.72	27.04 ± 0.65	0.05 ± 0.09	1.83 ± 0.92	88.9	77.2	4.6	−1.5	0.72	U,sl
$14^h03^m17^s$	279.3587	125.83 ± 1.50	-71.64 ± 0.29	31.46 ± 2.24	0.00 ± 0.02	7.31 ± 0.96	96.0	79.5	44.9	+0.9	0.79	U,sl
<median>	*279.27*§	*119.3 ± 4.9*	*−70.8 ± 1.8*	*30.5 ± 1.4*	*0.04 ± 0.06*	*0.13 ± 2.69*	*96.0*	*82.4*	*44.9*	*+1.2*	*0.68*	*U,sl*
$10^h34^m37^s$	280.2162	121.92 ± 0.25	-71.74 ± 0.07	30.87 ± 0.09	0.04 ± 0.03	0.04 ± 0.13	96.7	78.0	72.1	−1.0	0.47	U,sl
$10^h38^m14^s$	280.2188	122.48 ± 0.51	-71.30 ± 0.14	28.84 ± 0.21	0.03 ± 0.03	0.09 ± 0.05	92.9	82.8	42.7	+0.6	0.79	U,sl

Table 1 – Trajectory and light curve of 21 Volantid meteors on 2015 December 31, and two on 2016 January 1. $\lambda_\odot$ = solar longitude (J2000); RA_∞ and Dec_∞ are the Right Ascension and Declination of the apparent radiant; V_∞ is the apparent entry speed; a_1 and a_2 are deceleration parameters (Jenniskens et al., 2011); H_b and H_e are the beginning and end height; Q is the convergence angle of planes between station and meteor; M_v is the absolute visual magnitude (for a distance of 100 km); F is the shape parameter of the light curve, being 0 when peaking at the beginning and 1 when peaking at the end; and a final letter describes the shape of the light curve.

† Errors in Right Ascension are given as $\Delta RA * cos(Dec)$; a_1 and a_2 are defined in Jenniskens et al. (2011).

†† Notes: U = U-shaped; V = flare, V-shaped; fr = fragmentation (end flare), wd = wide; sl = slow rise.

§ Solar longitude at peak of the shower (accuracy $\sim \pm 0.^\circ 003$).

Table 1 – (continued) – geocentric radiant and orbital elements. RA, Dec, and V are now corrected for Earth's rotation and gravitational attraction. q = perihelion distance; a = semi-major axis; e = eccentricity, i = inclination, ω = argument of perihelion, Ω = node, Π = longitude of perihelion (J2000).

$\lambda_\odot$ (°)	RA_g (°)	Dec_g (°)	V_g (km/s)	q (AU)	$1/a$ (1/AU)	a (AU)	e	i (°)	ω (°)	Ω (°)	Π (°)
279.160	120.09 ± 0.76	-72.43 ± 0.61	30.43 ± 0.10	0.974 ± 0.002	0.313 ± 0.011	3.19	0.695 ± 0.011	49.92 ± 0.17	347.68 ± 1.09	99.1457 ± 0.0002	86.82 ± 1.09
279.166*	125.10 ± 0.78	-75.06 ± 0.19	29.95 ± 0.12	0.963 ± 0.001	0.351 ± 0.008	2.85	0.662 ± 0.007	49.31 ± 0.14	341.63 ± 0.57	99.1526 ± 0.0003	80.78 ± 0.57
279.181	126.24 ± 0.54	-71.16 ± 0.39	30.06 ± 0.07	0.974 ± 0.001	0.414 ± 0.007	2.42	0.597 ± 0.007	50.65 ± 0.14	347.27 ± 0.79	99.1669 ± 0.0002	86.43 ± 0.79
279.188	116.20 ± 1.37	-72.85 ± 0.98	29.13 ± 0.24	0.974 ± 0.003	0.343 ± 0.020	2.92	0.666 ± 0.019	47.84 ± 0.32	347.68 ± 1.84	99.1751 ± 0.0004	86.86 ± 1.84
279.197	123.20 ± 1.33	-73.44 ± 0.56	26.15 ± 0.28	0.969 ± 0.003	0.551 ± 0.015	1.81	0.466 ± 0.014	44.89 ± 0.35	342.43 ± 1.59	99.1845 ± 0.0005	81.61 ± 1.59
279.199*	114.12 ± 2.30	-74.25 ± 1.61	23.56 ± 0.30	0.970 ± 0.006	0.591 ± 0.019	1.69	0.427 ± 0.018	40.46 ± 0.43	342.90 ± 2.80	99.1869 ± 0.0006	82.09 ± 2.80
279.200*	114.91 ± 3.40	-74.83 ± 2.35	26.29 ± 0.20	0.969 ± 0.008	0.465 ± 0.031	2.15	0.550 ± 0.018	43.94 ± 0.30	343.37 ± 2.73	99.1870 ± 0.0003	82.56 ± 2.73
279.209	120.89 ± 14.61	-71.95 ± 3.37	28.17 ± 1.74	0.975 ± 0.022	0.449 ± 0.095	2.23	0.562 ± 0.091	47.49 ± 2.15	347.25 ± 9.54	99.1964 ± 0.0019	86.45 ± 9.54
279.211	120.90 ± 4.10	-71.42 ± 1.85	24.95 ± 0.76	0.975 ± 0.008	0.608 ± 0.039	1.64	0.407 ± 0.037	43.47 ± 1.02	346.41 ± 5.57	99.1984 ± 0.0012	85.61 ± 5.57
279.224	114.66 ± 1.00	-69.81 ± 1.04	28.39 ± 0.33	0.981 ± 0.002	0.394 ± 0.022	2.54	0.613 ± 0.022	47.26 ± 0.37	353.20 ± 2.07	99.2112 ± 0.0006	92.41 ± 2.07
279.228*†	—	—	—	—	—	—	—	—	—	—	—
279.242*†	—	—	—	—	—	—	—	—	—	—	—
279.269	126.04 ± 0.50	-66.44 ± 0.55	28.34 ± 0.18	0.983 ± 0.001	0.565 ± 0.013	1.77	0.445 ± 0.011	49.59 ± 0.29	355.83 ± 1.50	99.2564 ± 0.0002	95.09 ± 1.50
279.275	129.28 ± 1.67	-68.96 ± 1.53	27.05 ± 0.53	0.977 ± 0.005	0.625 ± 0.029	1.60	0.389 ± 0.029	47.80 ± 0.80	347.88 ± 3.93	99.2622 ± 0.0007	87.15 ± 3.93
279.298	113.12 ± 0.54	-71.99 ± 0.76	26.64 ± 0.31	0.977 ± 0.002	0.453 ± 0.019	2.21	0.557 ± 0.018	44.64 ± 0.39	349.12 ± 1.34	99.2867 ± 0.0002	88.40 ± 1.34
279.304	122.92 ± 0.40	-73.36 ± 0.43	27.88 ± 0.07	0.970 ± 0.001	0.466 ± 0.007	2.15	0.548 ± 0.008	47.07 ± 0.14	343.91 ± 0.72	99.2917 ± 0.0001	83.20 ± 0.72
279.316	123.65 ± 0.41	-70.54 ± 0.87	28.36 ± 0.41	0.977 ± 0.002	0.484 ± 0.025	2.07	0.527 ± 0.025	48.40 ± 0.52	348.76 ± 1.61	99.3039 ± 0.0004	88.06 ± 1.61
279.326	115.91 ± 0.77	-70.50 ± 0.75	29.34 ± 0.21	0.979 ± 0.001	0.350 ± 0.016	2.85	0.657 ± 0.016	48.47 ± 0.28	351.89 ± 1.35	99.3144 ± 0.0001	91.21 ± 1.35
279.343	124.11 ± 0.35	-71.91 ± 0.37	29.27 ± 0.13	0.973 ± 0.001	0.424 ± 0.009	2.36	0.587 ± 0.009	49.25 ± 0.20	346.61 ± 0.63	99.3316 ± 0.0000	85.94 ± 0.63
279.353*†	—	—	—	—	—	—	—	—	—	—	—
279.359	124.11 ± 17.81	-72.64 ± 4.54	29.43 ± 2.60	0.972 ± 0.019	0.406 ± 0.153	2.46	0.606 ± 0.149	49.26 ± 3.47	345.49 ± 7.03	99.3469 ± 0.0030	84.83 ± 7.03
<median>	*122.9 ± 4.7*	*-71.9 ± 1.9*	*28.4 ± 1.5*	*0.975 ± 0.004*	*0.449 ± 0.095*	*2.23*	*0.562 ± 0.093*	*47.8 ± 2.0*	*347.7 ± 3.4*	*99.256 ± 0.066*	*86.8 ± 3.4*
280.216	124.71 ± 0.56	-72.67 ± 0.34	28.72 ± 0.10	0.971 ± 0.001	0.452 ± 0.007	2.21	0.561 ± 0.007	48.54 ± 0.13	345.04 ± 0.74	100.2169 ± 0.0002	85.26 ± 0.74
280.219	125.63 ± 1.07	-72.31 ± 0.69	26.53 ± 0.24	0.971 ± 0.003	0.572 ± 0.015	1.75	0.445 ± 0.015	45.95 ± 0.32	343.75 ± 1.64	100.2199 ± 0.0003	83.97 ± 1.64

† Large uncertainty due to uncertain deceleration profile, data omitted.

Table 1 summarizes the results of these 23 trajectories, including 6 that were not so precisely measured and would normally be rejected (marked "*"). Those are not included in calculating the median values. On December 31, the radiants clustered around the apparent radiant RA = $119\overset{\circ}{.}3 \pm 4\overset{\circ}{.}9$, Dec = $-70\overset{\circ}{.}8 \pm 1\overset{\circ}{.}8$, with apparent speed $V_\infty = 30.5 \pm 1.4$ km/s (number of meteors $N = 15$), in the constellation of Volans (genitive Volantis). First introduced as "Pisces Volans" on star maps by Dutch cartographer Petrus Plancius in 1598, the name translates as "the flying fish".

The geocentric radiant was calculated at: RA = $122\overset{\circ}{.}9 \pm 4\overset{\circ}{.}7$, Dec = $-71\overset{\circ}{.}9 \pm 1\overset{\circ}{.}9$, and speed $V_g = 28.4 \pm 1.5$ km/s in the same constellation. The corresponding orbital elements are given in Table 1. The type of elements suggests a source that is a Jupiter-family comet, with relatively high inclination of $i = 48°$ and aphelion at 3.5 ± 0.9 AU.

The camera system is efficient at detecting bright meteors in the survey area, but only a fraction of fainter meteors are triangulated. Of all 4 230 meteors observed so far, the observed number distribution of -1 to -4 magnitude meteors is exponential, $N(m) \sim \chi^m$, with a fitted magnitude distribution index $\chi = 2.49 \pm 0.10$. From extrapolating this exponential distribution and comparing to the actual observed number of meteors fainter than -1 magnitude, we have a detection probability $P(m) = 1.00$, 1.00, 0.997, 0.753, 0.288, 0.046, and 0.002 for magnitudes -2 and up.

On December 31, the number of Volantids detected in each magnitude interval $m_v = -2, -1, \ldots +3$ is: 1, 2, 3, 8, 5 and 2. After correction for detection probability, the magnitude distribution index of the Volantids is $\chi = 2.17 \pm 0.17$ ($s = 1.84 \pm 0.08$). Hence, the new shower was relatively rich in bright meteors compared to all observed meteors. The magnitude distribution index is typical for a particle size distribution resulting from a collisional cascade ($\chi \sim 2.15$) with all meteoroids having the same strength against impacts (Jenniskens, 2006, p. 95). Meteoroids presumably collided efficiently during the ejection process.

An interesting feature of the stream is that all meteor light curves have a very similar shape, with a classic profile: an exponential increase, broad maximum and rapid decrease (Figure 3, right panel). The peak brightness is just past the center of the time interval. The brightest members show irregular light fluctuations at the peak (Figure 3). The beginning heights (Table 1) are typical of meteoroids from Jupiter-family comets entering at this speed.

The shower was active on more than one night. No Volantids were detected in the nights prior, but the yield was low: 6 total meteors on December 28, 3 on December 29 and none on December 30. The shower did continue into the new year. Two Volantids were detected in the next night of 2016 January 1, out of only three total (Table 1). Because of bad weather, no meteors were detected on January 2, and only one sporadic on January 3.

The shower may not be this active in other years. The shower was not detected by CAMS New Zealand in the previous year (Figure 3). The night of 2014 December 31, was mostly clear, but because of mist or condensation on the window only two meteors were detected. None were Volantids. The next night of 2015 January 1, was also clear between $\lambda_\odot$ = 280.44–280.70, with no haze this time. Of 44 detected meteors, none were Volantids. The shower is not listed by McIntosh (1935), nor by past radar observers (Nilsson, 1964; Gartrell & Elford, 1975).

We examined the orbital evolution of the individual meteoroids listed in Table 1 backwards for 10 000 years. We used the Mercury integrator (Chambers, 1999) and included all eight planets. The meteoroids did not approach the planets close enough to undergo considerable direct planetary perturbations. The simulations show that these particles were likely observed at the high inclination and low eccentricity phase of a Kozai cycle from secular perturbations. Note how inclination and perihelion distance oscillate (Figure 4). The period of this oscillation varies significantly from one meteoroid to the next, perhaps because of mean motion resonances. Of the 18 particles integrated, five were found to be librating in Jovian mean motion resonances at the present time: meteoroids #1, #4, #10, #13, and #16 are in the 9:4, 7:3, 3:1, 7:2 and 5:2 resonances, respectively. It is possible that this is just a result of measurement uncertainty in the semi-major axis (which range from 1.84–2.82 AU). However, the strong 3:1 and 5:2 resonances at 2.5 and 2.82 AU may well play a role in the evolution of the observed Volantid meteoroid stream. A non-annual shower can be caused by meteoroids trapped in a mean-motion resonance (Asher & Izumi, 1998; Jenniskens, 2006).

Until now, no parent body has been identified. The parent body is likely a Jupiter-family comet with a semi-major axis of 2.5 ± 0.3 AU. Its highly inclined orbit may have the same Kozai-cycle oscillations of q, e, i and Ω, so the parent comet could now be moving in an orbit with a significantly different inclination and perihelion distance.

Acknowledgements

We thank the reviewers Petr Pokorny and Javor Kac for their careful comments. CAMS is supported by the NASA Near Earth Object Observation program.

References

Asher D. and Izumi K. (1998). "Taurid swarm appearing in 1998?". *WGN, Journal of the IMO*, **26:5**, 217.

Chambers J. E. (1999). "A hybrid symplectic integrator that permits close encounters between massive bodies". *Mon. Not. of the Royal Astron. Soc.*, **304**, 793–799.

Ellyett C. D., Keay C. S. L., Roth K. W., and Bennett R. G. T. (1961). "The identification of meteor showers with application to southern hemisphere results". *MNRAS*, **123**, 37–50.

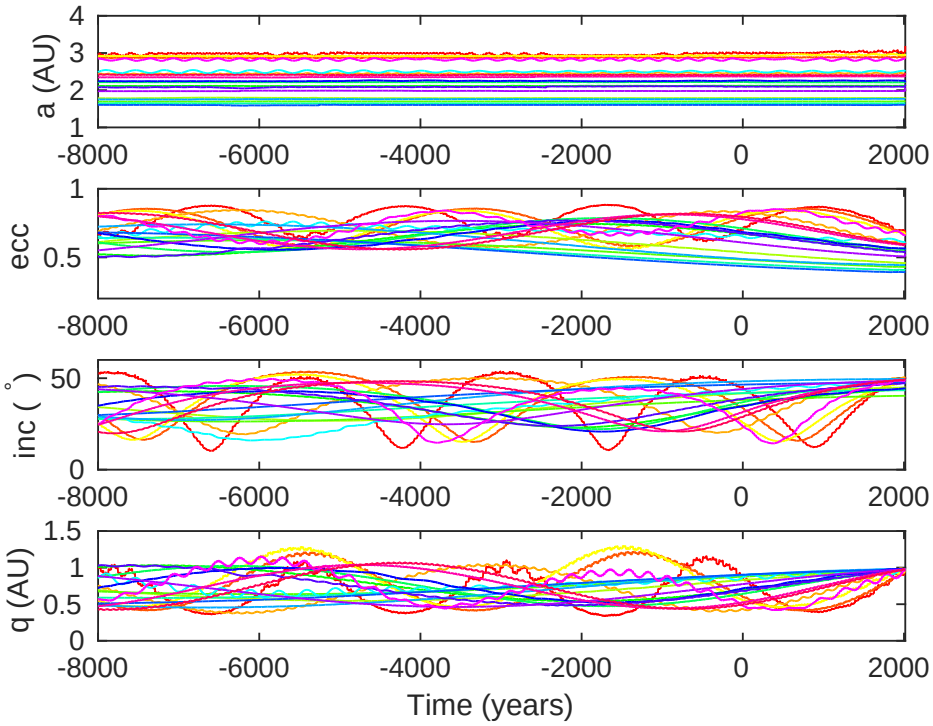

Figure 4 – Backwards integration of the orbits of observed Volantid meteors for 10 000 years.

Ellyett C. D. and Roth K. W. (1955). "The radar determination of meteor showers in the southern hemisphere". *Australian J. Phys.*, **8**, 390–401.

Galligan D. P. (2003). "Radar meteoroid orbit stream searches using cluster analysis". *MNRAS*, **340**, 899–907.

Galligan D. P. and Baggaley W. J. (2005). "The radiant distribution of AMOR radar meteors". *MNRAS*, **359**, 551–560.

Gartrell G. and Elford W. G. (1975). "Southern hemisphere meteor stream determination". *Austalian J. Phys.*, **28**, 591–620.

Janches D., Close S., Hormaechea J. L., Swarnalingam N., Murphy A., O'Connor D., Vandepeer B., Fuller B., Fritts D. C., and Brunini C. (2015). "The Southern Argentina Agile Meteor Radar Orbital System (SAAMER-OS): An initial sporadic meteoroid orbital survey in the southern sky". *Astrophys. J.*, **809**, 36–52.

Janches D., Hormaechea J. L., Brunini C., Hocking W., and Fritts D. C. (2013). "An initial meteoroid stream survey in the southern hemisphere using the SOuthern Argentina Agile Meteor Radar (SAAMER)". *Icarus*, **223**, 677–683.

Jenniskens P. (2006). *Meteor Showers and their Parent Comets*. Cambridge University Press, 790 pages.

Jenniskens P., Gural P. S., Dynneson L., Grigsby B., Newman K. E., Borden M., Koop M., and Holman D. (2011). "CAMS: Cameras for Allsky Meteor Surveillance to establish minor meteor showers". *Icarus*, **216**, 40–61.

Jenniskens P., Nénon Q., Gural P. S., Albers J., Haberman B., Johnson B., Morales R., Grigsby B. J., Samuels D., and Johannink C. (2016). "CAMS newly detected meteor showers and the sporadic background". *Icarus*, **266**, 384–409.

Jopek T. J., Koten P., and Pecina P. (2010). "Meteoroid streams identification among 231 southern hemisphere video meteors". *MNRAS*, **404**, 867–875.

McIntosh R. A. (1935). "An index to southern meteor showers". *MNRAS*, **95**, 709–718.

Molau S. and Kerr S. (2014). "Meteor showers of the southern hemisphere". *WGN, Journal of the IMO*, **42**, 68–75.

Nilsson C. S. (1964). "A southern hemisphere radio survey of meteor streams". *Astralian J. Phys.*, **17**, 205–256.

Poole L. M. G. (1995). "Meteor radiant distributions observed from Grahamstown, South Africa". *Earth, Moon and Planets*, **68**, 451–464.

Younger J. P., Reid I. M., Vincent R. A., Holdsworth D. A., and Murphy D. J. (2009). "A southern hemisphere survey of meteor shower radiants and associated stream orbits using single station radar observations". *MNRAS*, **398**, 350–356.

Handling Editor: Javor Kac

Observation error propagation on video meteor orbit determination

SonotaCo[1]

A new radiant direction error computation method on SonotaCo Network meteor observation data was tested. It uses single station observation error obtained by reference star measurement and trajectory linearity measurement on each video, as its source error value, and propagates this to the radiant and orbit parameter errors via the Monte Carlo simulation method. The resulting error values on a sample data set showed a reasonable error distribution that makes accuracy-based selecting feasible. A sample set of selected orbits obtained by this method revealed a sharper concentration of shower meteor radiants than we have ever seen before. The simultaneously observed meteor data sets published by the SonotaCo Network will be revised to include this error value on each record and will be publically available along with the computation program in near future.

Received 2016 January 25

1 Introduction

The identification of a meteor shower set is dependent on there being a sufficient number of low-biased orbits that have higher accuracy than natural distribution of shower meteors. Developments in automated video meteor observation systems have made possible long term observation with high constancy and continuity. The SonotaCo Network, which has been operating for over 9 years, holds over one and half million single station observations. From these, over 200 000 orbits have been determined from simultaneously observed meteors and were published as SonotaCo Network simultaneously observed meteor data sets (SNM) (SonotaCo, 2016). For these observations, problems of bias that affect optical meteor observation, due to weather conditions, lunar phase and the night time solar longitude range, are now almost overcome. However, the measurement accuracy problem has not yet been solved satisfactorily. In 2014, however, for the data processing of a new meteor shower, the April alpha Capricornids (IAU#752 AAC), a new radiant error computation method was tried and this showed a quite reasonable standard deviation of radiant direction (SonotaCo et al., 2014). If the uncertainty for each orbit could be stored in a large database, we would be able to select orbits according to their accuracy and this would produce a sharper map of the radiant. Thus the plan was to implement the new error propagation function on our orbit computation tool UFOOrbitV2 (UO2) (SonotaCo, 2007b). This paper describes the method and the result of its evaluation using a subset of SonotaCo Network data base.

2 Past approach

In general, the uncertainty of computed results should be determined from the mathematical error propagation of measurement error. On the SonotaCo Network, single station measurement software UFOAnalyzerV2 (UA2) (SonotaCo, 2007a), the observation error was automatically measured on each event by using the reference stars on the same video. However, error propagation is not carried out because there are least square methods in the reducing process on which the error propagation using covariance computation is difficult. Instead of error propagation, UO2 has provided some quality selection methods, such as threshold on duration or cross angle. These were effective in rejecting orbits of very low accuracy, but were not sufficient to sharpen the concentrations of shower meteors. Although CAMS (Jenniskens et al., 2011), uses assumed observation error, error propagation is carried out using the Monte Carlo simulation method and the uncertainties in the results were estimated. Hence, although it may require large quantity of computation, Monte Carlo simulation based on the actual observation error was expected to produce reliable uncertainty on SonotaCo Network data.

3 Observation error

The most dominant error factor in video meteor observation is the error in the determination of center direction of the bright object's image. Experimentally, the weighted center computation using the brightness of pixels on a video field gives around 10% of object's diameter. Hence there can be a method that uses the assumed uncertainty (such as 0.3 pixel) as the source error value. For this experiment, however, we tried to use the actually measured error values of each observation. This error appears both in the reference star position measurement and the meteor position measurement. On UA2, the former error is called FOV adjustment error d (expressed as "ddeg" on UA2) and is measured on each video as the average distance distance of each imaged reference fixed star from its star catalog position. To have the generality on the variety of FOV size and resolution, all measured positions in pixels are first converted to equatorial coordinate directions in degrees and the computations are all performed on these. This conversion uses 11 plate parameters including parameters for lens distortion, focus plane curvature, optical center offset, and pixel X/Y aspect ratio and so on. On a typical clear night, there are 50 to 100 reference stars automatically recognized on each video, and d is typically 0.°01 to 0.°1 (0.°01 corresponds to 0.1 pixel of 60° FOV NTSC system). The latter error is called trajectory linearity error c (expressed as "cdeg" on UA2) and is measured as the residual on the least square method of straight line fitting to the observed trajectory (com-

[1]SonotaCo Network, Toru Kanamori 2-11-6 Daizawa Setagaya-ku Tokyo 1550032, Japan.
Email: admin@sonotaco.jp

IMO bibcode WGN-442-sonotaco-error
NASA-ADS bibcode 2016JIMO...44...42S

putation of a plane that contains trajectory line and observing point). It depends on the size of the luminescence of a meteor, and c is typically in the range $0\overset{\circ}{.}01$ to $0\overset{\circ}{.}1$. The actual distribution of these values can be known from published SNM. These two values with the number of reference stars are included in the network hub data and also in the output of UO2. They have been stacked since 2007. For this experiment, the summation of both observation error on each meteor $e = d + c$ was used as the source observation error value for the error propagation.

4 Error Propagation

There are multiple observation factors that may dominate the final error in the orbit determination process. The major factors are, duration time (number of video frames), physical distance from the station to the meteor trajectory, cross angle among the simultaneous observation planes (geographical relation among stations and the meteor trajectory), and the singular point effect of velocity when it is near to the escape velocity of solar system and that of the Earth. The dominant factor is different for each meteor, and any of them can amplify the observational error up to infinity. Cross interaction among the factors also exists. In this complex situation, the usual error propagation using variance or covariance is very difficult, but the Monte Carlo simulation method with enough number of trials will produce the appropriate error values on the results.

For this experiment, the whole propagation process was divided into two stages. One involved the computation of observation plane pole for single station data, and the other involved the remaining part of the radiant and orbit computation using multi station data. The reason for this division was to fix the error of each single station result that might be used in multiple combination among the simultaneous observations. In the implementation of Monte Carlo method, to ensure the recomputability, the seed of artificial random numbers is fixed for each stage of each meteor. In each stage, 1000 times computations using random error on input were performed, and the standard deviation of the outputs were computed over the 1000 results obtained. And finally, as the accuracy measure, the standard deviation of the angle distance around the mean radiant direction Er was computed for each orbit. Er shows the uncertainty of radiant direction by one value, and it does not have scale bias like the Right Ascension error that has scale dependency on the Declination.

5 Evaluation on an actual sample

Sample data set

The evaluation of this new method was performed using a subset of actual SonotaCo Network observation data. The subset included all meteors that were observed in 1° solar longitude range of $283\overset{\circ}{.}0$ to $284\overset{\circ}{.}0$ over 10 years (2007 to 2016). It is the peak period of the Quadrantid (QUA) shower. This included data for 16 374 single station observations. Of these, 7047 were simultaneous observations and by applying the same quality conditions on UO2 as in the usual SNM determination, a data set S of 2662 meteor orbits with error values was obtained. Figure 1 shows the major part of its distribution of radiants.

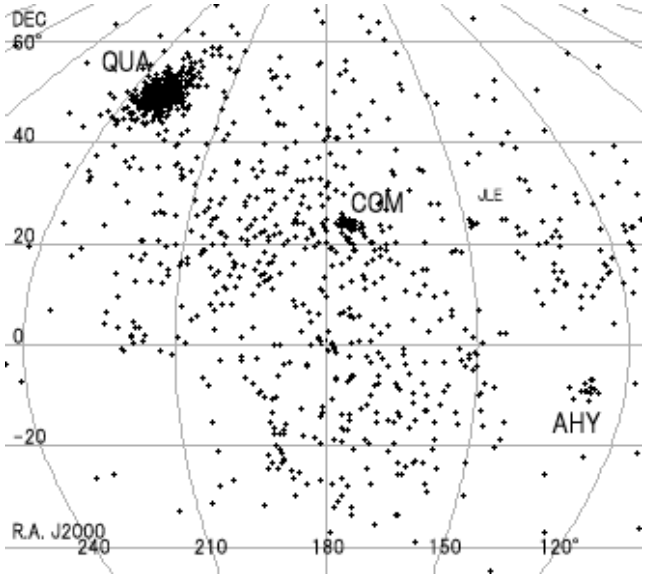

Figure 1 – All radiants in $\lambda_\odot$ range $283\overset{\circ}{.}0$ to $284\overset{\circ}{.}0$ over a 10 year period.

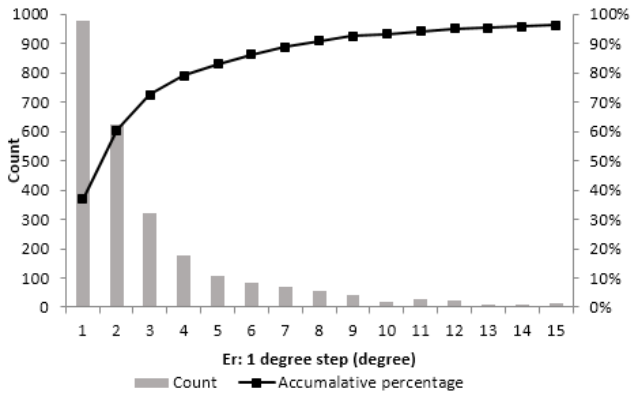

Figure 2 – Distribution of radiant error Er on sample data set.

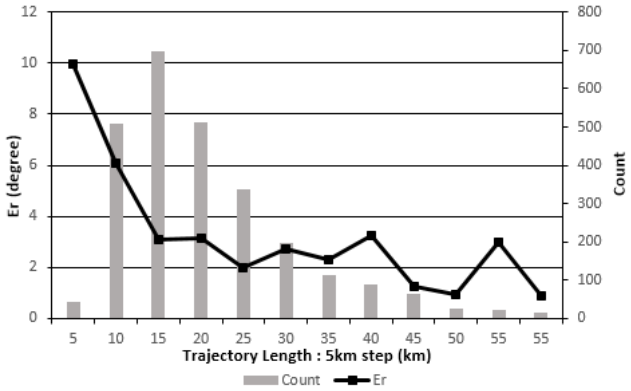

Figure 3 – Correlation between Er and the trajectory length.

Er distribution

Figure 2 shows the Er distribution of S. It shows that for 90% this was under 8°, and for 60% was under 2°.

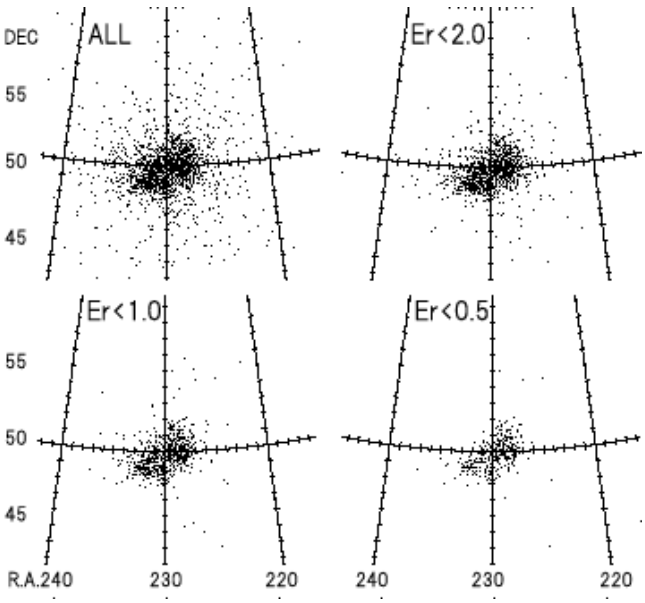

Figure 4 – Concentration of QUA shower meteors.

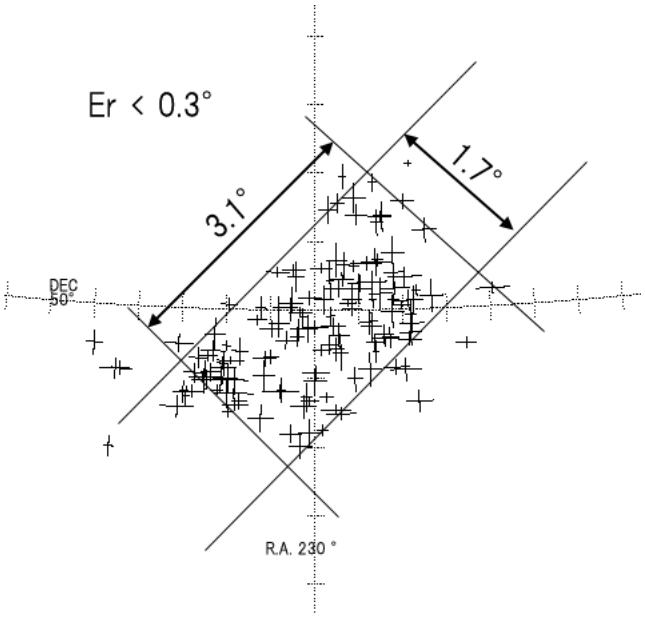

Figure 5 – QUA Radiant distribution on $1^\circ\lambda_\odot$ range.

This matches well with the impression that we have experienced for the multiple results computation with simultaneous observations from more than 2 stations. It also suggests that if we set an upper error threshold of 2°, we will still get over 130 000 precise orbits from 10 years of our observations.

Correlation between Er and error source factor

As a sample of correlation between Er and an error source factor, Figure 3 shows the correlation between meteor trajectory length and Er. It shows clear correlation where $Er > 3\,\overset{\circ}{.}0$. This means that the rejection of too short trajectories is effective for rejecting the orbits that have very poor accuracy. It also illustrates the difficulty in selecting high accuracy results, such as $Er < 2\,\overset{\circ}{.}0$, based on a single source factor.

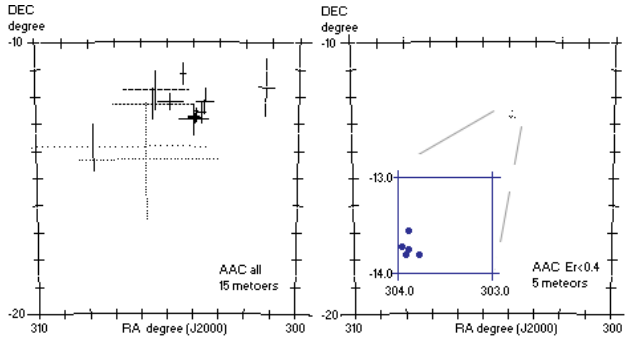

Figure 6 – Er restriction on April alpha Capricornids meteors.

Limitation of Er

If Er is properly expressing the observational uncertainty, and the uncertainty is not significantly smaller than that of the natural distribution of shower meteors, then selection on the results using the limitation of Er will sharpen the concentration of shower meteor distribution. Figures 4 and 5 show the QUA meteor shower concentration for some Er limits. The sharpness of the concentration is increasing along with the decrease of error limit. It is relatively clear on $Er > 1\,\overset{\circ}{.}0$, but still continues down to $Er > 0\,\overset{\circ}{.}3$. And finally we reached the $1\,\overset{\circ}{.}7 \times 3\,\overset{\circ}{.}1$ natural distribution of QUA meteor radiants of 1° $\lambda_\odot$ range. This result encourages us to use the Er value for the future research. For example, if we adopt this method to the AAC meteor shower from 2014, we get $0\,\overset{\circ}{.}3 \times 0\,\overset{\circ}{.}4$ radiant area at $Er < 0\,\overset{\circ}{.}4$ that is shown in Figure 6. This might be one of the most compact shower radiants concentration that we have ever seen. Figure 7 shows the result of $Er < 1\,\overset{\circ}{.}0$ limitation on S. Comparing with Figure 1, the limitation clearly sharpens the concentrations of shower meteors.

For these samples, the orbit selection using Er looks very effective and promising. We can use appropriate Er limit according to the purpose of the research. We should, however, be careful about the possibility of the observation bias that this selection might cause.

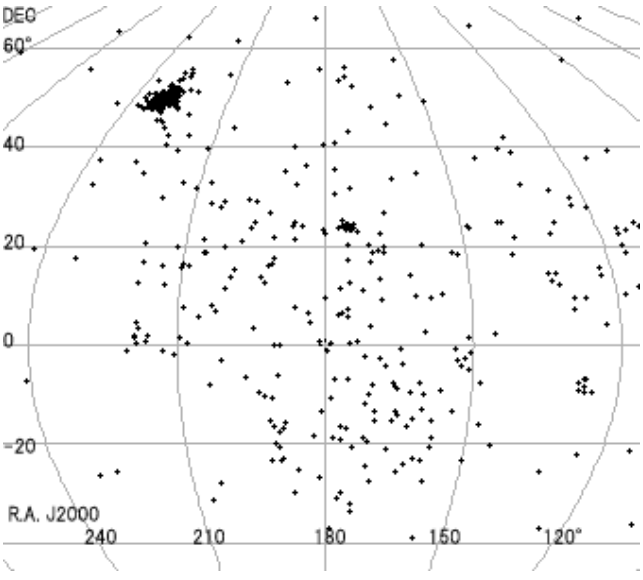

Figure 7 – Selected radiants $Er < 1\,\overset{\circ}{.}0$ on S.

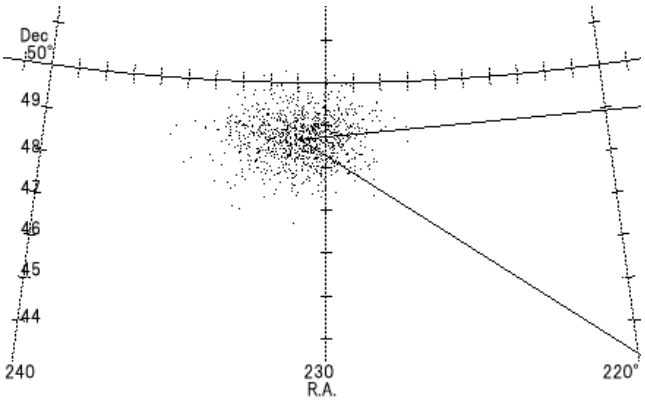

Figure 8 – Typical simulated error distribution of an actual meteor (20130103_114512, $Er = 1\overset{\circ}{.}02$).

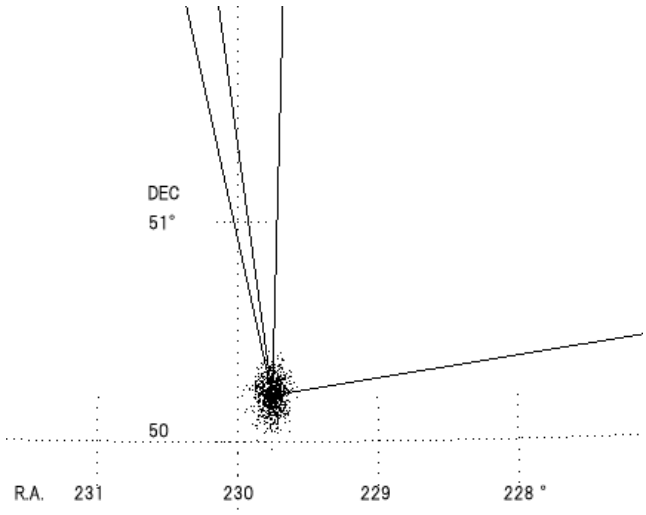

Figure 9 – Simulated error distribution of a highly accurate observation (20120104_152829, $Er = 0\overset{\circ}{.}09$).

It might be bias on the trajectory length, or objects weight.

Simulated Error Distribution

Figure 8 shows the typical simulated error distribution around the observed radiant. It is an actual sample of one QUA meteor (2013 January 3 at $11^{\rm h}45^{\rm m}12^{\rm s}$ UT, $Er = 1\overset{\circ}{.}02$, σRA $= 1\overset{\circ}{.}33$, σDec $= 0\overset{\circ}{.}54$). There are 1000 plots of simulated results and two straight lines showing the observed trajectory direction of each station. The cross angle between two trajectory directions was $37\overset{\circ}{.}8$, and there is small anisotropy along with the common trajectory direction. This sample suggests that too small a cross angle always results in a anisotropic distribution.

Figure 9 shows another sample for a highly accurate observation (2012 January 4 at $15^{\rm h}28^{\rm m}29^{\rm s}$ UT, $Er = 0\overset{\circ}{.}09$, σRA $= 0\overset{\circ}{.}06$, σDec $= 0\overset{\circ}{.}06$). This meteor was observed by 4 stations simultaneously. The distances from the trajectory to the stations are almost identical and are less than 200 km. The cross angle of trajectory direction among the stations is over 88°. It was an almost ideal case. However, some anisotropy can still be seen. It seems that 3 observations from one side (along with the Dec axis) might contribute to narrow the distribution of that direction (UO2 utilizes all simultaneous observation by least square method to decide the observed radiant).

These samples suggest that the anisotropy of error distribution around the radiant can happen depending on the cross angle or any asymmetricity on each observation.

6 Conclusions

The observation error propagation shows a reasonable error distribution that can be used for the effective selection of orbits. The selected orbits of actual shower meteors shows a very sharp concentration that we could not have seen before. The new error computation method can be adopted not only for newly observed orbits, but also for the large quantity of stored SonotaCo Network data, and is expected to produce many new findings. The updated version of UFOOrbitV2 that contains this error propagation function will be made publically available in near future with the updated SNM data base that has error values for each orbit.

We now have the final piece of an automated video meteor observation system. It will show us the precise distribution of actual Earth colliding objects. SonotaCo Network activity on the internet over 10 years, has now achieved one of its scientific goals.

Acknowledgements

Without the large quantity of observations by the SonotaCo Network members, nothing would have happened. Its observation accuracy is increasing year by year. It is the result of observers' continuous efforts. I give my fullest appreciation and respect for the observers who are listed in the SNM note files.

References

Jenniskens P., Gural P. S., Dynneson L., Grigsby B. J., Newman K. E., Borden M., Koop M., and Holman D. (2011). "CAMS: Cameras for Allsky Meteor Surveillance to establish minor meteor showers". *Icarus*, **216:1**, 40–61.

SonotaCo (2007a). "UFOAnalyzerV2 Users Manual". `http://sonotaco.com/soft/download/UA2Manual229.pdf` .

SonotaCo (2007b). "UFOOrbitV2 Users Manual". `http://sonotaco.com/soft/UO2/UO21Manual_JP.pdf` .

SonotaCo (2007-2016). "SonotaCo Network Simultaneously Observed Meteor Data Sets (SNM20xx)". `http://sonotaco.jp/doc/SNM/index.html` .

SonotaCo, Shimoda C., Inoue H., Masuzawa T., and Sato M. (2014). "Observation of April alpha Capricornids (IAU#752 AAC)". *WGN, Journal of the IMO*, **42:6**, 222–226.

Handling Editor: Javor Kac

Preliminary results

Results of the IMO Video Meteor Network — November 2015

Sirko Molau[1], *Stefano Crivello*[2], *Rui Goncalves*[3], *Carlos Saraiva*[4], *Enrico Stomeo*[5], *and Javor Kac*[6]

The November 2015 report of IMO Video Meteor Network observations is presented, covering more than 12 000 hours of observations with over 57 000 meteors being recorded. The flux density of the Northern Taurids is presented and follows the profile from the years 2011–2014. The flux density profile of the Southern Taurids is up to twice the average level from the years 2011–2014 between $\lambda_\odot$ 212° and 235°. The flux density profile is also presented for the Leonids for the period 2011–2015.

Received 2016 March 10

1 Introduction

In October 2015, the record-breaking year took a short rest. After we obtained one record after the other, the preceding month was rather modest. The more prominent November showed its superiority.

Looking at the observing statistics we note larger gaps, but November is not a summer month and considering that, the output was extraordinary. The best night was November 4/5, when 73 of 82 cameras were active. 51 cameras managed to observe in twenty or more nights, and many of these had to pause in no more than two or three nights. In particular in south European countries like Spain or Italy the observers enjoyed perfect observing conditions, but also in Germany where this month is renowned for dirty weather. When skies were clear, it was often for the full night, such that in total more than 12 000 hours of effective observing time could be collected (Table 1 and Figure 1). That is a third more than in the previously best November 2011, and the second best result in the entire history of the IMO Network. The meteor yield was even better. We recorded over 57 000 meteors which is an increase of 60% compared to 2011. For the first time since the Leonid storm of 2001, November provided more meteors than the two preceding months.

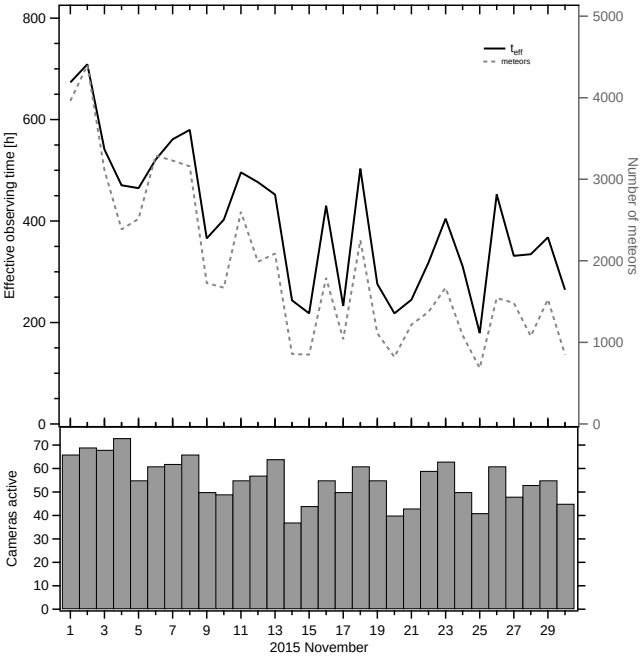

Figure 1 – Monthly summary for the effective observing time (solid black line), number of meteors (dashed gray line) and number of cameras active (bars) in 2015 November.

2 Taurid fireballs

Particularly remarkable was the time until November 8, when we recorded between 2 000 and 4 000 meteors each night. Readers of the IMO Meteor Shower Calendar (McBeath, 2014) and other predictions will immediately think of the Taurids. Model calculations by Asher & Clube (1993) had predicted the return of the "Taurid swarm" in 2015. The last observed swarm in 2005 showed increased fireball activity in the last three days of October and the first third of November (McBeath, 2014). That is a particularly active segment of the Taurids which also comes along with many fireballs. Indeed the last October night was accompanied by a brilliant Taurid fireball that was well observed in East Germany, and also in the neighboring countries (Figure 2).

Via the AKM fireball report form we received almost a hundred reports in a few days, in the end we were contacted by 141 eye witnesses. Since Sirko Molau receives an e-mail for every incoming report, his mailbox quickly filled. When the stream of reports continued for several days he started to wonder why casual observers from the public would report their sightings only a week after the event. So he had a closer look and was surprised to learn that these reports belonged to ever newer fireballs! Only after mid-November the stream of reports petered out suddenly.

Figure 3 shows how many different events were reported via the fireball report form in October and

[1]Abenstalstr. 13b, 84072 Seysdorf, Germany.
Email: sirko@molau.de
[2]Via Bobbio 9a/18, 16137 Genova, Italy.
Email: stefano.crivello@libero.it
[3]Urbanizacao da Boavista, Lote 46, Linhaceira, 2305-114 Asseiceira, Tomar, Portugal. Email: rui.goncalves@ipt.pt
[4]Rua Aquilino Ribeiro, 23 - 1 Dto. 2790028 Carnaxide, Portugal. Email: carlos.saraiva@netcabo.pt
[5]via Umbria 21/d, 30037 Scorze (VE), Italy.
Email: stom@iol.it
[6]Na Ajdov hrib 24, 2310 Slovenska Bistrica, Slovenia.
Email: javor.kac@orion-drustvo.si

IMO bibcode WGN-442-molau-vidnov
NASA-ADS bibcode 2016JIMO...44...46M

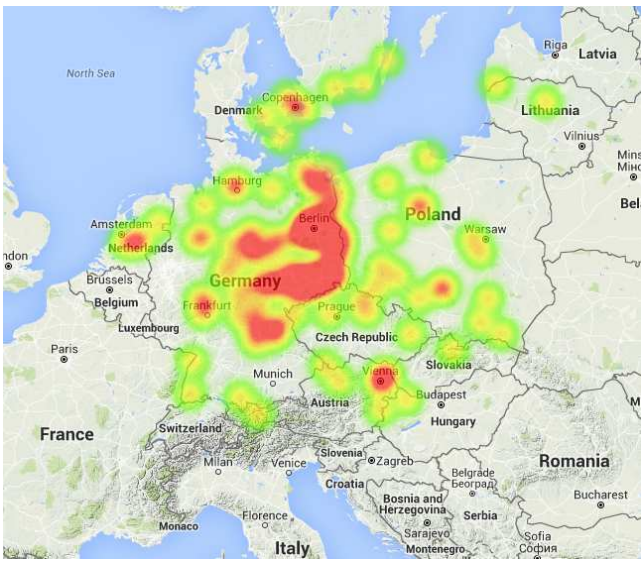

Figure 2 – "Heat map" of the fireball on 2015 October 31, at 18^h06^m UT over East Germany. The plot represents 141 observing reports that were received via the fireball report form of AKM and IMO.

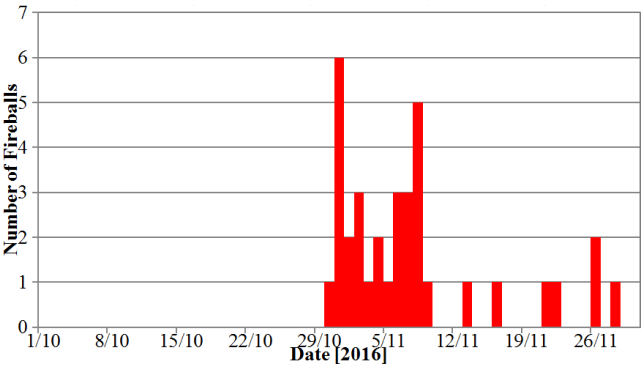

Figure 3 – Number of fireball events that were reported in October and November 2015 from observers in Germany via the fireball report forms of AKM and IMO.

November. The analysis is not highly professional as it does not account for the weather, for example. Still it confirms remarkably, that the predicted high fireball rate due to the Taurid swarm had materialized. In total we counted 35 fireballs with over 370 individual reports!

Now the question was, whether the activity of "ordinary" Taurids that we observe with our video cameras was affected in the same way? The flux density of the Northern Taurids was within the usual boundaries, whereas the activity of the Southern Taurids was well above the typical level (Figure 4).

The deviation is even more prominent in Figure 5, where we compare the flux density profile of 2015 with the average profile of the last four years. The outlier at 215° solar longitude can be ignored, since the data set from that night is insufficient. We see that the Northern Taurids follow their long-term trend with the activity starting only a few days earlier. The Southern Taurids, however, show up to twice the normal activity between 212° and 235° solar longitude (October 25 to November 17) if we subtract the constant background (sporadic chance alignments).

We analysed the population index between October 20 and November 20 utilizing the same algorithm as in

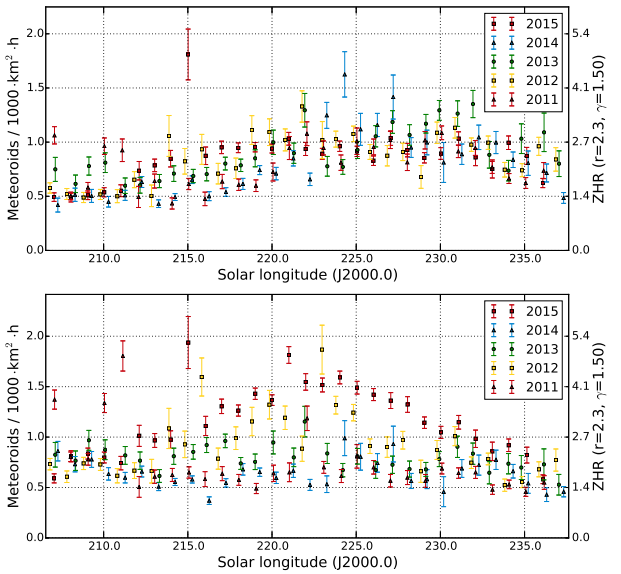

Figure 4 – Comparison of the flux density profile of the Northern (top) and Southern Taurids (bottom) in 2015 and in the preceding years, derived from observations of the IMO Video Network.

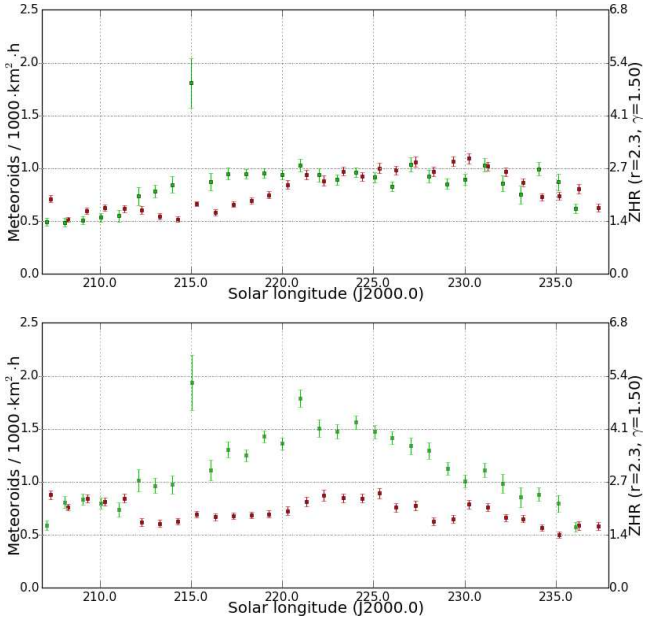

Figure 5 – Comparison of the flux density profile of the Northern (top) and Southern Taurids (bottom) in 2015 (green) and in the preceding years (red).

the previous months including the perception coefficient correction. We did not account for the long-term trend (e.g. affected by the lunar phase) because the sporadic meteors did not provide an adequate data set.

Figure 6 shows the population index profile for the Northern and Southern Taurids. Both showers present a flat profile, with little deviations in the first third of November. The mean population index of both showers was 2.2.

Particularly interesting is a massive dip of the r-value on October 30/31. This dip is also prominent in the combined profile, where all Taurids were pooled into one shower (Figure 7, top). Thanks to the larger meteor count, the scatter in this plot is even smaller. The r-value decreases by 0.6 in that night. Disenchanting is

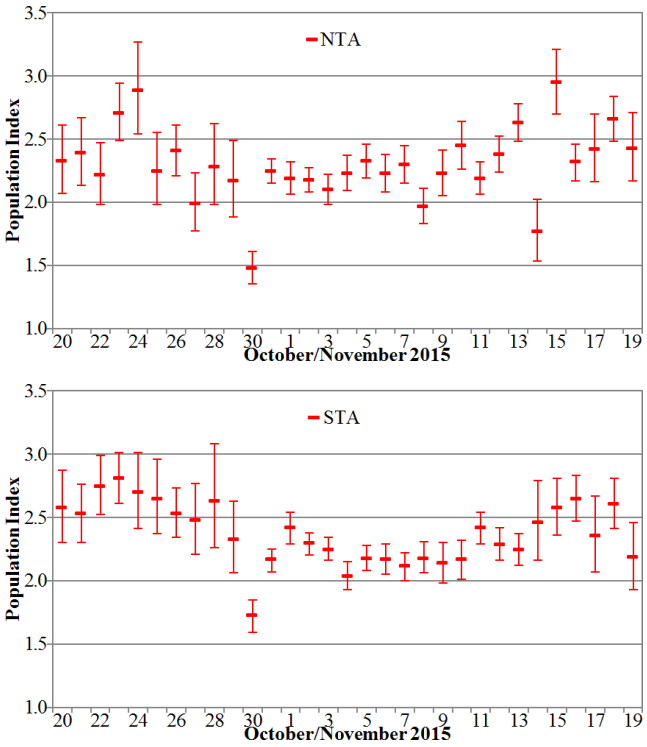

Figure 6 – Population index profile of the Northern (top) and Southern Taurids (bottom) in October/November 2015.

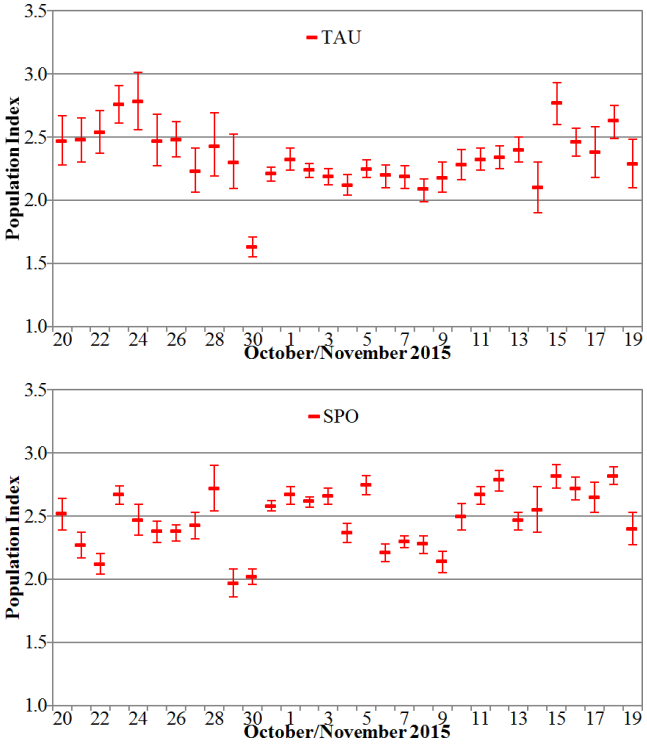

Figure 7 – Population index profile of the Taurids (top) and sporadic meteors (bottom) in 2015 October/November.

a look at the sporadic r-profile (Figure 7, bottom). It shows much larger variations than the Taurid profile, but particularly on October 29/30 and 30/31 this profile also shows a significant dip of about −0.6.

So we can only conclude that the r-value of the Taurids is 0.4 smaller than the sporadic population index in the first days of November (Figure 8). However, there

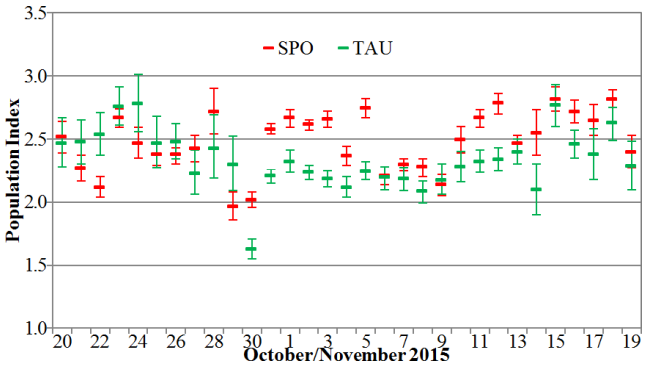

Figure 8 – Comparison of the population index profile of the Taurids and sporadic meteors in 2015 October/November.

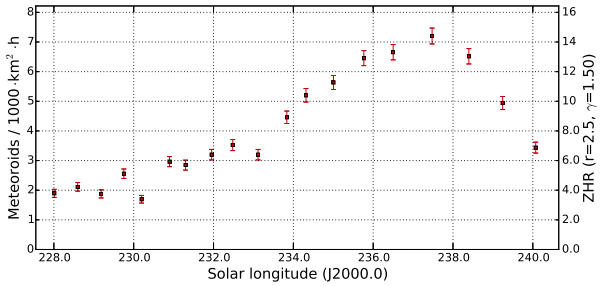

Figure 9 – Averaged flux density profile of the Leonids 2011–2015, derived from observations of the IMO Video Network.

are further hints of an unusual brightness distribution on October 30/31. The percentage of Taurids which was recorded by cameras with poor limiting magnitude and large fields of view was typically smaller than or equally large as the percentage of the most sensitive cameras. Only in that particular October night, the weaker cameras were much more successful in recording Taurids than on other nights.

3 Other showers of November

Beside the Taurids, there were no spectacular events in November. Neither the Leonids nor the α-Monocerotids provided surprises. Both showers presented the same activity profile as in the years before – the Leonids had distinct activity whereas the α-Monocerotids were hardly detectable. Figure 9 shows the average profile of the Leonids from 2011 to 2015. The activity starts to grow at 230° solar longitude. With 7 meteoroids per 1 000 km^2 per hour, the largest flux density is reached at 237°, and then the activity falls back to the original level within four days.

References

Asher D. J. and Clube S. V. M. (1993). "An extraterrestrial influence during the current glacial-interglacial". *Quarterly Journal of the Royal Astronomical Society*, **34:4**, 481–511.

McBeath A. (2014). "2015 Meteor Shower Calendar". International Meteor Organization. IMO INFO(2-14).

Handling Editor: Javor Kac

Code	Name	Location	Camera	FOV [°²]	Stellar LM [mag]	Eff.CA [km²]	Nights	Time [h]	Meteors
ARLRA	Arlt	Ludwigsfelde/DE	Ludwig2 (0.8/8)	1475	6.2	3779	25	122.1	762
BANPE	Bánfalvi	Zalaegerszeg/HU	Huvcse01 (0.95/5)	2423	3.4	361	21	55.5	424
BERER	Berkó	Ludányhalászi/HU	Hulud1 (0.8/3.8)	5542	4.8	3847	18	151.5	943
BOMMA	Bombardini	Faenza/IT	Mario (1.2/4.0)	5794	3.3	739	19	134.1	807
BREMA	Breukers	Hengelo/NL	Mbb3 (0.75/6)	2399	4.2	699	9	40.1	131
BRIBE	Klemt	Herne/DE	Hermine (0.8/6)	2374	4.2	678	14	84.1	337
		Bergisch Gladbach/DE	Klemoi (0.8/6)	2286	4.6	1080	18	74.9	322
CASFL	Castellani	Monte Baldo/IT	Bmh1 (0.8/6)	2350	5.0	1611	28	288.6	1290
			Bmh2 (1.5/4.5)*	4243	3.0	371	29	295.2	1085
CRIST	Crivello	Valbrevenna/IT	Bilbo (0.8/3.8)	5458	4.2	1772	29	184.0	1048
			C3P8 (0.8/3.8)	5455	4.2	1586	25	128.8	547
			Stg38 (0.8/3.8)	5614	4.4	2007	28	195.5	1589
CSISZ	Csizmadia	Baja/HU	Huvcse02 (0.95/5)	1606	3.8	390	21	131.2	328
DONJE	Donani	Faenza/IT	Jenni (1.2/4)	5886	3.9	1222	21	180.7	1110
ELTMA	Eltri	Venezia/IT	Met38 (0.8/3.8)	5631	4.3	2151	16	152.3	692
FORKE	Förster	Carlsfeld/DE	Akm3 (0.75/6)	2375	5.1	2154	16	103.0	555
GONRU	Goncalves	Tomar/PT	Templar1 (0.8/6)	2179	5.3	1842	27	263.2	1300
			Templar2 (0.8/6)	2080	5.0	1508	27	271.9	1144
			Templar3 (0.8/8)	1438	4.3	571	27	257.7	600
			Templar4 (0.8/3.8)	4475	3.0	442	27	265.8	1142
			Templar5 (0.75/6)	2312	5.0	2259	27	250.1	1210
GOVMI	Govedič	Središče ob Dravi/SI	Orion2 (0.8/8)	1447	5.5	1841	22	184.8	944
			Orion3 (0.95/5)	2665	4.9	2069	20	149.7	377
			Orion4 (0.95/5)	2662	4.3	1043	23	183.3	462
HERCA	Hergenrother	Tucson/US	Salsa3 (0.8/3.8)	2336	4.1	544	29	282.1	987
HINWO	Hinz	Schwarzenberg/DE	Hinwo1 (0.75/6)	2291	5.1	1819	19	118.4	677
IGAAN	Igaz	Debrecen/HU	Hudeb (0.8/3.8)	5522	3.2	620	15	120.3	307
		Hódmezővásárhely/HU	Huhod (0.8/3.8)	5502	3.4	764	18	72.1	246
		Budapest/HU	Hupol (1.2/4)	3790	3.3	475	7	49.1	37
JONKA	Jonas	Budapest/HU	Husor (0.95/4)	2286	3.9	445	24	182.4	447
			Husor2 (0.95/3.5)	2465	3.9	715	24	176.8	422
KACJA	Kac	Ljubljana/SI	Orion1 (0.8/8)	1402	3.8	331	23	149.0	314
		Kamnik/SI	Cvetka (0.8/3.8)*	4914	4.3	1842	20	185.6	1358
			Rezika (0.8/6)	2270	4.4	840	21	200.6	2353
			Stefka (0.8/3.8)	5471	2.8	379	22	180.7	1159
		Kostanjevec/SI	Metka (0.8/12)*	715	6.4	640	2	21.5	120
KOSDE	Koschny	Izana Obs./ES	Icc7 (0.85/25)*	714	5.9	1464	26	216.9	1905
			Lic1 (2.8/50)*	2255	6.2	5670	20	134.4	1757
		La Palma/ES	Icc9 (0.85/25)*	683	6.7	2951	28	194.2	1366
		Noordwijkerhout/NL	Lic4 (1.4/50)*	2027	6.0	4509	11	43.3	106
LOJTO	Łojek	Grabniak/PL	Pav57 (1.0/5)	1631	3.5	269	8	56.9	117
LOPAL	Lopes	Lisbon/PT	Naso1 (0.75/6)	2377	3.8	506	4	7.8	56

Table 1 – Observers contributing to 2015 November data of the IMO Video Meteor Network. Eff.CA designates the effective collection area; the overall number of nights is the number of nights with at least one camera operating, the overall observing time and number of meteors are sums over all cameras.

Table 1 – Observers contributing to 2015 November data of the IMO Video Meteor Network – continued from previous page.

Code	Name	Location	Camera	FOV [°²]	Stellar LM [mag]	Eff.CA [km²]	Nights	Time [h]	Meteors
MACMA	Maciejewski	Chełm/PL	Pav35 (0.8/3.8)	5495	4.0	1584	19	95.2	544
			Pav36 (0.8/3.8)*	5668	4.0	1573	19	97.9	481
			Pav43 (0.75/4.5)*	3132	3.1	319	16	102.8	358
			Pav60 (0.75/4.5)	2250	3.1	281	18	107.0	523
MARGR	Maravelias	Lofoupoli-Crete/GR	Loomecon (0.8/12)	738	6.3	2698	22	177.2	668
MARRU	Marques	Lisbon/PT	Cab1 (0.8/3.8)	5291	3.1	467	29	257.6	1107
			Ran1 (1.4/4.5)	4405	4.0	1241	27	249.8	912
MOLSI	Molau	Seysdorf/DE	Avis2 (1.4/50)*	1230	6.9	6152	28	185.7	1843
			Escimo2 (0.85/25)	155	8.1	3415	25	180.5	338
			Mincam1 (0.8/8)	1477	4.9	1084	27	150.9	957
		Ketzür/DE	Remo1 (0.8/8)	1467	6.5	5491	25	131.5	747
			Remo2 (0.8/8)	1478	6.4	4778	25	135.1	680
			Remo3 (0.8/8)	1420	5.6	1967	16	84.8	364
			Remo4 (0.8/8)	1478	6.5	5358	21	124.8	736
MORJO	Morvai	Fülöpszállás/HU	Huful (1.4/5)	2522	3.5	532	23	163.2	392
MOSFA	Moschini	Rovereto/IT	Rover (1.4/4.5)	3896	4.2	1292	26	73.3	484
OCHPA	Ochner	Albiano/IT	Albiano (1.2/4.5)	2944	3.5	358	3	22.4	54
OTTMI	Otte	Pearl City/US	Orie1 (1.4/5.7)	3837	3.8	460	7	38.6	152
PERZS	Perkó	Becsehely/HU	Hubec (0.8/3.8)*	5498	2.9	460	23	193.8	1282
ROTEC	Rothenberg	Berlin/DE	Armefa (0.8/6)	2366	4.5	911	13	78.1	141
SARAN	Saraiva	Carnaxide/PT	Ro1 (0.75/6)	2362	3.7	381	26	229.2	626
			Ro2 (0.75/6)	2381	3.8	459	25	279.4	958
			Ro3 (0.8/12)	710	5.2	619	24	263.5	981
			Sofia (0.8/12)	738	5.3	907	26	266.4	765
SCALE	Scarpa	Alberoni/IT	Leo (1.2/4.5)*	4152	4.5	2052	10	79.9	171
SCHHA	Schremmer	Niederkrüchten/DE	Doraemon (0.8/3.8)	4900	3.0	409	22	103.3	476
SLAST	Slavec	Ljubljana/SI	Kayak1 (1.8/28)	563	6.2	1294	23	179.7	745
			Kayak2 (0.8/12)	741	5.5	920	22	197.0	383
STOEN	Stomeo	Scorze/IT	Min38 (0.8/3.8)	5566	4.8	3270	20	169.5	1151
			Noa38 (0.8/3.8)	5609	4.2	1911	20	173.2	1052
			Sco38 (0.8/3.8)	5598	4.8	3306	21	170.9	1279
STORO	Štork	Ondřejov/CZ	Ond1 (1.4/50)*	2195	5.8	4595	1	2.0	9
STRJO	Strunk	Herford/DE	Mincam2 (0.8/6)	2354	5.4	2751	19	82.0	479
			Mincam3 (0.8/6)	2338	5.5	3590	18	83.6	400
			Mincam4 (1.0/2.6)	9791	2.7	552	17	29.8	82
			Mincam5 (0.8/6)	2349	5.0	1896	18	79.3	328
			Mincam6 (0.8/6)	2395	5.1	2178	18	81.2	284
TEPIS	Tepliczky	Agostyán/HU	Huago (0.75/4.5)	2427	4.4	1036	25	170.7	518
			Humob (0.8/6)	2388	4.8	1607	23	159.7	762
YRJIL	Yrjölä	Kuusankoski/FI	Finexcam (0.8/6)	2337	5.5	3574	7	53.5	274
* active field of view smaller than video frame						Overall	30	12 044.2	57 369

Results of the IMO Video Meteor Network — December 2015

Sirko Molau[1], *Stefano Crivello*[2], *Rui Goncalves*[3], *Carlos Saraiva*[4], *Enrico Stomeo*[5], *and Javor Kac*[6]

In 2015 December, 80 cameras of the IMO Video Meteor Network recorded over 60 000 meteors in more than 10 600 hours of observing time. The flux density profile is presented for the Geminids and compared to previous years. The population index profile of the Geminids is also presented. The activity of the Ursids was slightly enhanced again. The flux density profile is presented and compared to profiles since 2011. The annual summary of the 2015 IMO Video Meteor Network observations is presented. More than 480 000 meteors were recorded in almost 122 000 hours of observing time.

Received 2016 April 12

1 Introduction

Statistics of December looked even spottier than in the preceding month, but still we obtained another record-breaking result. 42 out of the 80 cameras observed in twenty or more observing nights, the two Italian cameras Bmh2 and Rover even in 31. But the observers were not only successful in southern Europe – also observers in Germany and Poland enjoyed favorable observing conditions. The Geminids provided their share to the overall outcome as well. Their maximum occurred in the European daytime hours of December 13, so that we enjoyed high rates both in the night before and thereafter. That was combined with a convenient lunar phase. At the Geminid peak, the moon was just three days old. Not all observers enjoyed clear skies in both nights, but when it cleared, the cameras recorded many hundreds of meteors. Number one of 2015 was Hulud1 of Erno Berko, which detected over 600 shooting stars on December 13/14. In the three nights of December 12–15 we recorded a total of 20 000 meteors.

With a total of more than 10 600 observing hours (Table 1 and Figure 1), we surpassed the previously best December outcome of 2013 by 10%. Over 60 000 meteors is an increase of more than a quarter compared to 2013. Detlef Koschny contributed particularly to this result, since all his intensified video cameras at the Canary Islands enjoyed perfect conditions and provided over 10 000 meteors in total.

2 Geminids

Let us turn towards the most important shower of the month – the Geminids. As in the years before (Molau et al., 2012; Molau et al., 2013; Molau et al., 2014; Molau et al., 2015) we had to select a higher zenith exponent of $\gamma = 1.7$ to flatten the flux density profile of the Geminids. Figure 2 shows the profile of the whole shower with a temporal resolution of ≥ 30 min per measurement. It is obvious that the Geminid peak was not covered by us in this year.

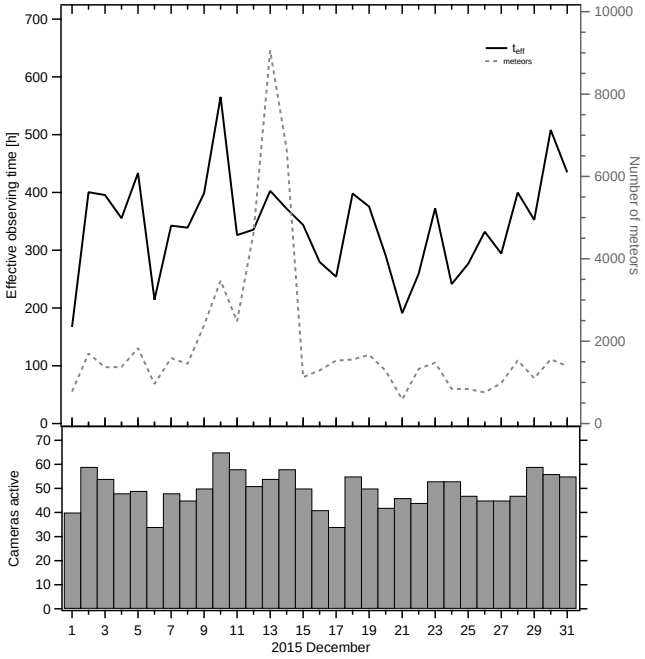

Figure 1 – Monthly summary for the effective observing time (solid black line), number of meteors (dashed gray line) and number of cameras active (bars) in 2015 December.

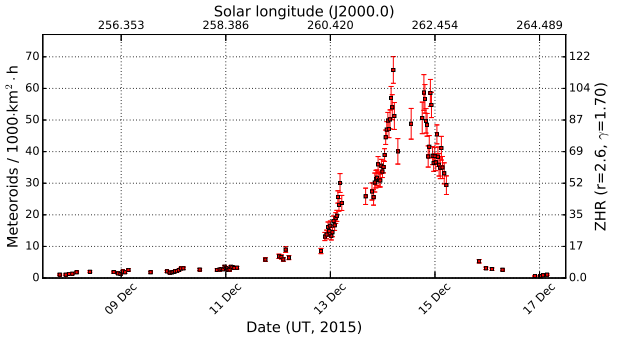

Figure 2 – Flux density profile of the Geminids 2015, derived from observations of the IMO Video Network.

For the December 11–16 section, Figure 3 presents a comparison of the last four years. We can see that the segments of the individual years fit quite well to each other. Only the transitions between the nights often do

[1]Abenstalstr. 13b, 84072 Seysdorf, Germany. Email: sirko@molau.de
[2]Via Bobbio 9a/18, 16137 Genova, Italy. Email: stefano.crivello@libero.it
[3]Urbanizacao da Boavista, Lote 46, Linhaceira, 2305-114 Asseiceira, Tomar, Portugal. Email: rui.goncalves@ipt.pt
[4]Rua Aquilino Ribeiro, 23 - 1 Dto. 2790028 Carnaxide, Portugal. Email: carlos.saraiva@netcabo.pt
[5]via Umbria 21/d, 30037 Scorze (VE), Italy. Email: stom@iol.it
[6]Na Ajdov hrib 24, 2310 Slovenska Bistrica, Slovenia. Email: javor.kac@orion-drustvo.si

IMO bibcode WGN-442-molau-viddec
NASA-ADS bibcode 2016JIMO...44...51M

Code	Name	Location	Camera	FOV [°²]	Stellar LM [mag]	Eff.CA [km²]	Nights	Time [h]	Meteors
ARLRA	Arlt	Ludwigsfelde/DE	Ludwig2 (0.8/8)	1475	6.2	3779	26	165.9	1394
BANPE	Bánfalvi	Zalaegerszeg/HU	Huvcse01 (0.95/5)	2423	3.4	361	12	26.1	251
BERER	Berkó	Ludányhalászi/HU	Hulud1 (0.8/3.8)	5542	4.8	3847	8	59.1	892
BOMMA	Bombardini	Faenza/IT	Mario (1.2/4.0)	5794	3.3	739	21	127.5	890
BREMA	Breukers	Hengelo/NL	Mbb3 (0.75/6)	2399	4.2	699	21	114.8	328
BRIBE	Klemt	Herne/DE	Hermine (0.8/6)	2374	4.2	678	23	154.7	519
		Bergisch Gladbach/DE	Klemoi (0.8/6)	2286	4.6	1080	21	159.0	507
CASFL	Castellani	Monte Baldo/IT	Bmh1 (0.8/6)	2350	5.0	1611	30	357.5	2008
			Bmh2 (1.5/4.5)*	4243	3.0	371	31	331.2	1677
CRIST	Crivello	Valbrevenna/IT	Bilbo (0.8/3.8)	5458	4.2	1772	19	104.2	676
			C3P8 (0.8/3.8)	5455	4.2	1586	16	100.1	405
			Stg38 (0.8/3.8)	5614	4.4	2007	20	127.2	1086
DONJE	Donani	Faenza/IT	Jenni (1.2/4)	5886	3.9	1222	19	117.0	895
ELTMA	Eltri	Venezia/IT	Met38 (0.8/3.8)	5631	4.3	2151	12	120.1	1116
FORKE	Förster	Carlsfeld/DE	Akm3 (0.75/6)	2375	5.1	2154	22	158.4	861
GONRU	Goncalves	Tomar/PT	Templar1 (0.8/6)	2179	5.3	1842	25	178.2	723
			Templar2 (0.8/6)	2080	5.0	1508	24	176.8	620
			Templar3 (0.8/8)	1438	4.3	571	22	145.6	280
			Templar4 (0.8/3.8)	4475	3.0	442	24	155.4	615
			Templar5 (0.75/6)	2312	5.0	2259	24	143.8	571
GOVMI	Govedič	Središče ob Dravi/SI	Orion2 (0.8/8)	1447	5.5	1841	18	142.9	514
			Orion3 (0.95/5)	2665	4.9	2069	18	75.3	140
			Orion4 (0.95/5)	2662	4.3	1043	20	128.5	256
HERCA	Hergenrother	Tucson/US	Salsa3 (0.8/3.8)	2336	4.1	544	29	270.6	864
HINWO	Hinz	Schwarzenberg/DE	Hinwo1 (0.75/6)	2291	5.1	1819	27	243.6	1255
IGAAN	Igaz	Debrecen/HU	Hudeb (0.8/3.8)	5522	3.2	620	7	58.0	177
		Hódmezővásárhely/HU	Huhod (0.8/3.8)	5502	3.4	764	6	32.8	86
JONKA	Jonas	Budapest/HU	Husor (0.95/4)	2286	3.9	445	13	64.3	258
			Husor2 (0.95/3.5)	2465	3.9	715	11	61.7	262
KACJA	Kac	Ljubljana/SI	Orion1 (0.8/8)	1402	3.8	331	15	72.7	141
		Kamnik/SI	Cvetka (0.8/3.8)*	4914	4.3	1842	21	145.0	1055
			Rezika (0.8/6)	2270	4.4	840	21	177.9	1995
			Stefka (0.8/3.8)	5471	2.8	379	19	137.6	872
		Kostanjevec/SI	Metka (0.8/12)*	715	6.4	640	1	5.3	17
KOSDE	Koschny	Izana Obs./ES	Icc7 (0.85/25)*	714	5.9	1464	26	189.4	1973
			Lic1 (2.8/50)*	2255	6.2	5670	17	128.6	2011
		La Palma/ES	Icc9 (0.85/25)*	683	6.7	2951	24	192.3	2959
			Lic2 (3.2/50)*	2199	6.5	7512	18	166.3	3041
		Noordwijkerhout/NL	Lic4 (1.4/50)*	2027	6.0	4509	14	61.8	126
LOJTO	Łojek	Grabniak/PL	Pav57 (1.0/5)	1631	3.5	269	11	77.7	278
LOPAL	Lopes	Lisbon/PT	Naso1 (0.75/6)	2377	3.8	506	9	58.4	51

Table 1 – Observers contributing to 2015 December data of the IMO Video Meteor Network. Eff.CA designates the effective collection area; the overall number of nights is the number of nights with at least one camera operating, the overall observing time and number of meteors are sums over all cameras.

Table 1 – Observers contributing to 2015 December data of the IMO Video Meteor Network – continued from previous page.

Code	Name	Location	Camera	FOV [°²]	Stellar LM [mag]	Eff.CA [km²]	Nights	Time [h]	Meteors
MACMA	Maciejewski	Chełm/PL	Pav35 (0.8/3.8)	5495	4.0	1584	25	137.3	811
			Pav36 (0.8/3.8)*	5668	4.0	1573	25	156.8	748
			Pav43 (0.75/4.5)*	3132	3.1	319	24	162.8	524
			Pav60 (0.75/4.5)	2250	3.1	281	27	171.7	823
MARGR	Maravelias	Lofoupoli-Crete/GR	Loomecon (0.8/12)	738	6.3	2698	18	48.0	473
MARRU	Marques	Lisbon/PT	Cab1 (0.8/3.8)	5291	3.1	467	16	122.7	474
			Ran1 (1.4/4.5)	4405	4.0	1241	18	123.4	454
MOLSI	Molau	Seysdorf/DE	Avis2 (1.4/50)*	1230	6.9	6152	28	210.2	1789
			Escimo2 (0.85/25)	155	8.1	3415	21	206.6	256
			Mincam1 (0.8/8)	1477	4.9	1084	24	188.2	1232
		Ketzür/DE	Remo1 (0.8/8)	1467	6.5	5491	25	171.7	1290
			Remo2 (0.8/8)	1478	6.4	4778	25	178.3	1459
			Remo3 (0.8/8)	1420	5.6	1967	20	133.5	647
			Remo4 (0.8/8)	1478	6.5	5358	22	122.6	720
MORJO	Morvai	Fülöpszállás/HU	Huful (1.4/5)	2522	3.5	532	10	72.2	137
MOSFA	Moschini	Rovereto/IT	Rover (1.4/4.5)	3896	4.2	1292	31	95.9	897
OTTMI	Otte	Pearl City/US	Orie1 (1.4/5.7)	3837	3.8	460	17	106.8	197
PERZS	Perkó	Becsehely/HU	Hubec (0.8/3.8)*	5498	2.9	460	18	125.5	1100
ROTEC	Rothenberg	Berlin/DE	Armefa (0.8/6)	2366	4.5	911	17	133.7	347
SARAN	Saraiva	Carnaxide/PT	Ro1 (0.75/6)	2362	3.7	381	20	126.6	313
			Ro2 (0.75/6)	2381	3.8	459	18	132.7	356
			Ro3 (0.8/12)	710	5.2	619	18	144.1	397
			Sofia (0.8/12)	738	5.3	907	17	131.6	273
SCALE	Scarpa	Alberoni/IT	Leo (1.2/4.5)*	4152	4.5	2052	15	110.7	466
SCHHA	Schremmer	Niederkrüchten/DE	Doraemon (0.8/3.8)	4900	3.0	409	23	118.8	468
SLAST	Slavec	Ljubljana/SI	Kayak1 (1.8/28)	563	6.2	1294	16	108.1	327
			Kayak2 (0.8/12)	741	5.5	920	14	115.6	211
STOEN	Stomeo	Scorze/IT	Min38 (0.8/3.8)	5566	4.8	3270	20	152.2	1421
			Noa38 (0.8/3.8)	5609	4.2	1911	19	157.4	1684
			Sco38 (0.8/3.8)	5598	4.8	3306	21	164.4	1701
STRJO	Strunk	Herford/DE	Mincam2 (0.8/6)	2354	5.4	2751	23	152.1	718
			Mincam3 (0.8/6)	2338	5.5	3590	25	147.4	496
			Mincam4 (1.0/2.6)	9791	2.7	552	20	49.8	128
			Mincam5 (0.8/6)	2349	5.0	1896	23	148.9	490
			Mincam6 (0.8/6)	2395	5.1	2178	20	136.3	370
TEPIS	Tepliczky	Agostyán/HU	Huago (0.75/4.5)	2427	4.4	1036	15	116.4	566
			Humob (0.8/6)	2388	4.8	1607	11	93.9	676
TRIMI	Triglav	Velenje/SI	Sraka (0.8/6)*	2222	4.0	546	5	52.8	82
YRJIL	Yrjölä	Kuusankoski/FI	Finexcam (0.8/6)	2337	5.5	3574	16	112.3	440
						Overall	31	10 653.3	60 606

* active field of view smaller than video frame

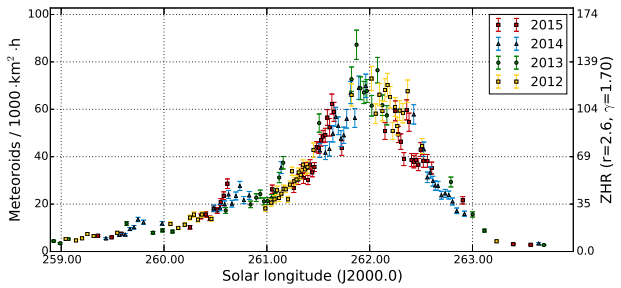

Figure 3 – Flux density profile of the Geminids 2012–2015, derived from observations of the IMO Video Network.

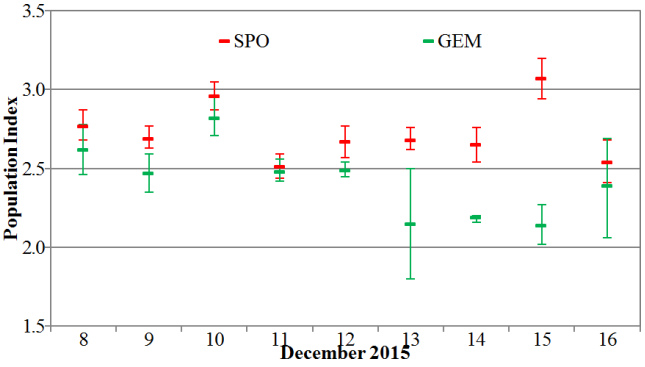

Figure 4 – Population index profile of the Geminids and sporadic meteors in December 2015.

not agree very well, even when the zenith exponent is adapted. That hints on the fact that the dependency of the flux density from the radiant altitude is more complex than the zenith exponent model. In particular at the end of a night, rates are often overestimated.

Figure 4 presents the population index for the activity period of the Geminids. For sporadic meteors the values scatters between $r = 2.6$ and 3.0. Until the night of December 12/13, the Geminids show virtually the same population index. Since their flux density is particularly low in the first few nights, the "sporadic dilution" is particularly strong there. With values near $r = 2.2$, the Geminid population index is clearly smaller than the sporadic r-value in the three following nights.

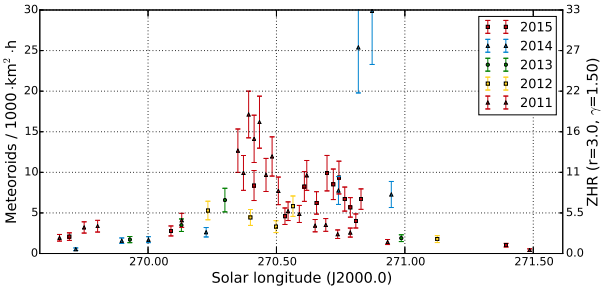

Figure 5 – Flux density profile of the Ursids 2011–2015, derived from observations of the IMO Video Network.

3 Ursids

From time to time the Ursids provide nice surprises just before Christmas. In 2011 we observed a flux density of up to 15 meteoroids per 1 000 km^2 per hour near 270°.4 solar longitude (Molau et al., 2012). The shower remained inconspicuous in 2012 and 2013 with peak flux densities of 5 (Molau et al., 2013; Molau et al., 2014). In 2014 we observed an even stronger outburst with up to 25 meteoroids per 1 000 km^2 per hour near 270°.8 solar longitude (Molau et al., 2015), when activity had already declined in the years before. In 2015 the activity was slightly enhanced again with rates up to 10 meteoroids per 1 000 km^2 per hour just below the peaks of 2011 and 2014. Hence, the peak activity and time of the Ursids varies from year to year similar to the Quadrantids a few days later.

4 2015 summary

Let us now make up a balance for 2015. The size of our camera network did not change, but thanks to the exceptional observing conditions we clearly outdid all the previous years. In the 17th year of the IMO Network, 48 observers (2014: 48) from 14 countries (2014: 15) contributed with 92 meteor cameras (2014: 92) to the network. In the competition between the countries, Germany is ahead with 19 cameras, followed by Hungary (17), Italy (13), Slovenia and Portugal (both 12).

Table 2 – Monthly distribution of video observations in the IMO Network 2015.

Month	Observing Nights	Eff. Observing Time	Meteors	Meteors / Hour
January	31	9 566.3	25 370	2.7
February	28	10 041.8	19 963	2.0
March	31	11 251.8	18 968	1.7
April	30	10 867.4	25 506	2.3
May	31	7 466.7	16 691	2.2
June	30	7 168.5	18 791	2.6
July	31	9 382.8	36 883	3.9
August	31	12 386.7	91 442	7.4
September	30	11 371.6	53 871	4.7
October	31	9 640.8	54 848	5.7
November	30	12 055.0	57 423	4.8
December	31	10 653.3	60 606	5.7
Overall	365	121 852.7	480 362	3.9

Table 3 – Distribution of video observations over the observers in 2015.

Observer	Country	Observing Nights	Eff. Observing Time [h]	Meteors	Meteors / h	Cameras (Stations)
Detlef Koschny	Netherlands	351	5 495.0	46 642	8.5	4 (3)
Sirko Molau	Germany	342	10 059.2	57 765	5.7	7 (2)
Rui Goncalves	Portugal	341	11 010.4	35 553	3.2	5 (1)
Carl Hergenrother	USA	330	2 568.9	6 570	2.6	1 (1)
Stefano Crivello	Italy	322	5 549.8	26 387	4.8	3 (1)
Rui Marques	Portugal	322	3 923.1	12 166	3.1	2 (1)
Flavio Castellani	Italy	308	4 341.2	15 590	3.6	2 (1)
Enrico Stomeo	Italy	307	5 206.9	31 820	6.1	3 (1)
Carlos Saraiva	Portugal	306	8 119.3	19 882	2.4	4 (1)
Jörg Strunk	Germany	300	6 233.0	18 194	2.9	4 (1)
Rainer Arlt	Germany	294	1 526.4	9 387	6.1	1 (1)
Maciej Maciejewski	Poland	292	5 831.6	26 469	4.5	4 (1)
Bernd Klemt	Germany	288	2 763.1	8 455	3.1	2 (2)
Jenni Donati	Italy	280	1 932.5	10 492	5.4	1 (1)
Istvan Tepliczky	Hungary	278	3 263.7	10 565	3.2	2 (1)
Mario Bombardini	Italy	276	1 701.1	8 129	4.8	1 (1)
Fabio Moschini	Italy	276	793.1	3 652	4.6	1 (1)
Antal Igaz	Hungary	274	3 417.4	6 274	1.8	3 (3)
Hans Schremmer	Germany	274	1 252.7	4 631	3.7	1 (1)
Javor Kac	Slovenia	264	5 003.5	26 214	5.2	5 (3)
Karoly Jonas	Hungary	259	2 916.0	5 767	2.0	1 (1)
Stane Slavec	Slovenia	257	2 798.2	5 371	1.9	2 (1)
Mitja Govedič	Slovenia	253	3 466.7	10 671	3.1	3 (1)
Zsolt Perkó	Hungary	253	1 652.3	7 856	4.8	1 (1)
József Morvai	Hungary	245	1 640.8	2 801	1.7	1 (1)
Mike Otte	USA	245	1 367.2	2 770	2.0	1 (1)
Maurizio Eltri	Italy	238	1 498.6	6 466	4.3	1 (1)
Wolfgang Hinz	Germany	237	1 470.7	6 678	4.5	1 (1)
Grigoris Maravelias	Greece	232	1 624.1	4 344	2.7	1 (1)
Martin Breukers	Netherlands	222	1 211.0	2 862	2.4	1 (1)
Kevin Förster	Germany	221	1 298.2	5 861	4.5	1 (1)
Eckehard Rothenberg	Germany	208	1 250.4	2 744	2.2	1 (1)
Szilárd Csizmadia	Hungary	194	962.4	2 016	2.1	1 (1)
Mihaela Triglav	Slovenia	189	675.6	1 947	2.9	1 (1)
Alvaro Lopes	Portugal	184	423.0	1 596	3.8	1 (1)
Péter Bánfalvi	Hungary	166	303.2	2 013	6.6	1 (1)
Szabolcs Kiss	Hungary	161	888.7	1 070	1.2	1 (1)
Rok Pucer	Slovenia	157	980.2	2 117	2.2	1 (1)
Erno Berkó	Hungary	148	1 702.4	8 734	5.1	1 (1)
Paolo Ochner	Italy	137	684.7	1 851	2.7	1 (1)
Leo Scarpa	Italy	135	718.3	2 172	3.0	1 (1)
Ilkka Yrjölä	Finland	132	803.5	2 947	3.7	1 (1)
Mikhail Maslov	Russia	128	533.8	2 129	4.0	1 (1)
Tomasz Lojek	Poland	117	684.2	1 361	2.0	1 (1)
Zoltán Zelko	Hungary	43	239.8	419	1.7	2 (1)
Rafael Schmall	Hungary	11	30.9	75	2.4	1 (1)
Rosta Štork	Czech Republic	5	32.9	883	26.8	2 (2)
Luc Bastiaens	Belgium	1	3.0	4	1.3	1 (1)

Further cameras were operated in Poland (5), Spain (4), the Netherlands, USA and Czech Republic (all 2), as well as Belgium, Greece, Finland and Russia (all 1).

In 365 observing nights (2014: 365) and 121 853 hours of effective observing time (2014: 99 880) we recorded 480 362 meteors (2014: 367 036). Thus, the effective observing time increased by over 20% relative to the previous best result, the meteor count even by more than 30%. With 3.9 meteors per hour we obtained the same average as in the three years before.

Table 2 shows the monthly distribution of observations. In seven individual months and also in the monthly average of 2015 we collected more than 10 000 observing hours. So far we achieved this in four months

Table 4 – The ten most successful video systems in 2015.

Camera	Location	Observer	Observing Nights	Eff. Observing Time [h]	Meteors	Meteors / h
Salsa3	Tucson (US)	Carl Hergenrother	330	2 568.9	6 570	2.6
Templar1	Tomar (PT)	Rui Goncalves	315	2 306.4	9 055	3.9
Templar2	Tomar (PT)	Rui Goncalves	311	2 303.5	7 384	3.2
Templar4	Tomar (PT)	Rui Goncalves	310	2 200.3	7 815	3.6
Templar5	Tomar (PT)	Rui Goncalves	309	2 078.4	7 596	3.7
Stg38	Valbrevenna (IT)	Stefano Crivello	303	2 033.1	12 675	6.2
Bilbo	Valbrevenna (IT)	Stefano Crivello	301	1 913.8	8 296	4.3
Templar3	Tomar (PT)	Rui Goncalves	295	2 121.8	3 703	1.7
Sco38	Scorze (IT)	Enrico Stomeo	295	1 800.7	11 657	6.5
Ludwig2	Ludwigsfelde (DE)	Rainer Arlt	294	1 526.4	9 387	6.1

only (2× 2014, 1× 2011 and 2012 each). Starting from August we recorded every month over 50 000 meteors, which we managed before 2015 only four times in August and two times in October. All the figures underline the superb observing conditions, but also the high quality and stability of the cameras in the IMO Network.

Under these conditions it is no surprise that also the number of observers with 300 and more observing nights increased from seven in 2014 to ten in 2015. Detlef Koschny made it to the top – with 351 observing nights he outdid the old record by Antal Igaz from 2012 by five nights. Sirko Molau increased his own record by eleven nights and obtained with 342 exactly one more night than Rui Goncalves. There was only little shift in the next positions, but Rui Marques, Flavio Castellani, Carlos Saraiva and Jörg Strunk managed for the first time to observe in over 300 nights. Further 22 observers obtained over 200 and 12 over 100 observing nights.

Regarding the effective observing time, Rui Goncalves defended the top rank for the fourth time. Sirko Molau and he collected for the first time over 10 000 observing hours in a single year, and also the third rank remained with Carlos Saraiva.

Regarding the meteor counts there was also no change in the first three places. With a record-breaking 58 000 meteors, Sirko Molau remained on top of the list, followed by Detlef Koschny and Rui Goncalves. Eleven more observers contributed over 10 000 meteors to the final outcome.

Table 3 summarizes the details for all active observers of the IMO Video Meteor Network. The number of cameras and stations refers to the majority of 2015.

In 2014, two cameras obtained more than 300 observing nights and 280 nights were sufficient to make it into the TOP-10. In 2015, the bar was further raised, since there were already 7 cameras with 300 or more nights. Salsa3 of Carl Hergenrother in Tucson/USA is leading this list by far. It is followed by all cameras of Rui Goncalves, as well as three Italian and one German camera. If the threshold was left at 280 nights, the list would have to be extended by twelve more entries.

Two of the TOP-10 cameras recorded more than 10 000 meteors, further eight are missing in the list: Icc9 (16 233), Icc7 (13 638), Avis2 (13 399), Lic1 (11 502), Remo1 (10 962), Rezika (10 890), Jenni (10 492) and Min38 (10 335).

The complete data set of the IMO Video Meteor Network including the 2015 data is now available for download at the homepage of the IMO Network `http://www.imonet.org`. Currently the database contains 2 614 295 meteors from 634 346 hours of effective observing time in 5 738 nights.

As always, we would like to thank the many observers, whose passion is a guarantor for the success of the IMO Network. Special thanks Stefano Crivello, Enrico Stomeo, Rui Goncalves, Carlos Saraiva, Maciej Maciejewski and Mikhail Maslov, who check together with Sirko Molau every month the consistency of the data set and ensure the high quality of the database. Even though it seems unlikely that we can obtain the same fantastic result in 2016 again, we keep our fingers crossed and wish clear skies to everyone.

References

Molau S., Kac J., Berko E., Crivello S., Stomeo E., Igaz A., and Barentsen G. (2012). "Results of the IMO Video Meteor Network – December 2011". *WGN, Journal of the IMO*, **40:2**, 69–75.

Molau S., Kac J., Berko E., Crivello S., Stomeo E., Igaz A., Barentsen G., and Goncalves R. (2013). "Results of the IMO Video Meteor Network – December 2012". *WGN, Journal of the IMO*, **41:2**, 52–60.

Molau S., Kac J., Crivello S., Stomeo E., Barentsen G., Goncalves R., and Igaz A. (2014). "Results of the IMO Video Meteor Network – December 2013". *WGN, Journal of the IMO*, **42:2**, 76–82.

Molau S., Kac J., Crivello S., Stomeo E., Barentsen G., Goncalves R., Saraiva C., Maciejewski M., and Maslov M. (2015). "Results of the IMO Video Meteor Network – December 2014". *WGN, Journal of the IMO*, **43:2**, 62–68.

Handling Editor: Javor Kac

The International Meteor Organization

web site http://www.imo.net

Council

President: Cis Verbeeck,
Bogaertsheide 5, 2560 Kessel, Belgium.
e-mail: cis.verbeeck@scarlet.be

Vice-President: Jürgen Rendtel,
Eschenweg 16, D-14476 Marquardt, Germany.
tel. +49 33208 50753
e-mail: jrendtel@aip.de

Secretary-General: Robert Lunsford,
1828 Cobblecreek Street, Chula Vista,
CA 91913-3917, USA. tel. +1 619 585 9642
e-mail: lunro.imo.usa@cox.net

Treasurer: Marc Gyssens, Heerbaan 74,
B-2530 Boechout, Belgium.
e-mail: marc.gyssens@uhasselt.be
BIC: GEBABEBB
IBAN: BE30 0014 7327 5911
Always state BIC and IBAN codes together!
Check international transfer charges with your bank; you are responsible for paying these.

Other Council members:

Megan Argo, Jodrell Bank Centre for Astrophysics, Alan Turing building, University of Manchester, Oxford Road, Manchester, M13 9PL, UK.
e-mail: megan.argo@gmail.com

Geert Barentsen, NASA Ames Research Center, M/S 244-30, Moffett Field CA 94035, USA.
e-mail: hello@geert.io

Javor Kac (see details under WGN)

Detlef Koschny, Zeestraat 46,
NL-2211 XH Noordwijkerhout, Netherlands.
e-mail: detlef.koschny@esa.int

Masahiro Koseki, 4-3-5 Annaka, Annaka-shi,
Gunma-ken 379-0116, Japan.
e-mail: geh04301@nifty.ne.jp

Sirko Molau, Abenstalstraße 13b, D-84072 Seysdorf, Germany. e-mail: sirko@molau.de

Jean-Louis Rault, Société Astronomique de France, 16, rue de la Vallée, 91360 Epinay sur Orge, France. e-mail: f6agr@orange.fr

Paul Roggemans, Pijnboomstraat 25, 2800 Mechelen, Belgium, e-mail: paul.roggemans@gmail.com

Galina Ryabova, Research Institute of Applied Mathematics and Mechanics of Tomsk State University, Lenin pr. 36, build. 27, 634050 Tomsk, Russian Federation.
e-mail: ryabova@niipmm.tsu.ru

Damir Šegon, J. Rakovca 3, 52100 Pula, Croatia. e-mail: damir.segon@pu.t-com.hr

Juraj Tóth, Faculty of Mathematics, Physics and Informatics, Comenius University in Bratislava, Mlynska dolina, 84248 Bratislava, Slovakia.
e-mail: toth@fmph.uniba.sk

Commission Directors

Visual Commission: Rainer Arlt (rarlt@aip.de)
Generic e-mail address: visual@imo.net
Electronic visual report form:
http://www.imo.net/visual/report/electronic

Video Commission: Sirko Molau (sirko@molau.de)
Generic e-mail address: video@imo.net

Photographic Commission: Bill Ward (William.Ward@glasgow.ac.uk)
Generic e-mail address: photo@imo.net

Radio Commission: Jean-Louis Rault (f6agr@orange.fr)
Generic e-mail address: radio@imo.net

Fireballs: Online fireball reports:
http://fireballs.imo.net

Outreach Officer

Jure Atanackov, e-mail: jureatanackov@gmail.com

Press Officer

Megan Argo, e-mail: megan.argo@gmail.com

WGN

Editor-in-chief: Javor Kac
Na Ajdov hrib 24, SI-2310 Slovenska Bistrica, Slovenia. e-mail: wgn@imo.net;
include METEOR in the e-mail subject line

Editorial board: Ž. Andreić, M. Argo, D.J. Asher, J. Correira, M. Gyssens, C. Hergenrother, T. Markham, J. Rendtel, J.-L. Rault, C. Verbeeck.

IMO Sales

Available from the Treasurer or the Electronic Shop on the IMO Website	€	$
IMO membership, including subscription to WGN Vol. 44 (2016)		
Surface mail	26	39
Air Mail (outside Europe only)	49	69
Electronic subscription only	21	29
Back issues of WGN on paper (price per complete volume)		
Vols. 26 (1998) – 35 (2007)	15	23
Vols. 37 (2009) – 43 (2015) – electronic version only	9	13
Proceedings of the International Meteor Conference on paper		
1990, 1991, 1993, 1995, 1996, 1999, 2000, 2002, 2003, per year	9	13
2007, 2010, 2011, per year	15	23
2012, 2013, 2014, 2015 per year	25	37
Proceedings of the Meteor Orbit Determination Workshop 2006	15	23
Radio Meteor School Proceedings 2005	15	23
Handbook for Meteor Observers	15	23
Meteor Shower Workbook	12	18
Electronic media		
Meteor Beliefs Project CD-ROM	6	9
DVD: WGN Vols. 6–30 & IMC 1991, 1993–96, 2001–04	45	69

Bright Fireball over South of the Netherlands on 2016 March 25

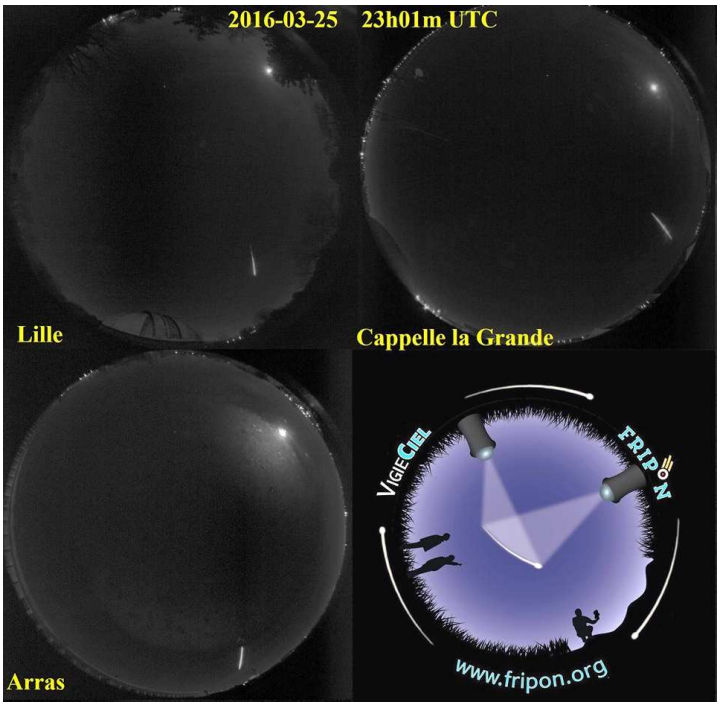

The International Meteor Organization received 70 reports about a fireball event over the Netherlands on 2016 March 25 around $23^{h}00^{m}$ UT. The fireball was seen primarily from Belgium and from the Netherlands but witnesses from France, Luxembourg and the UK also reported the event (map below). Allsky cameras of the Fripon network (top left) also captured the event. The fireball was best documented by Klaas Jobse from Oostkapelle, the Netherlands. The top right image was obtained using Watec 902H2 Ultimate, 1.2 mm lens and UFOCapture, while the image on the right was taken with a Canon 400D equipped with a 4.5 mm fish eye lens, and exposed from $22^{h}59^{m}15^{s}$ to $23^{h}01^{m}15^{s}$ UT. The brightest flare reached magnitude -12 as seen from Oostkapelle.